Research Paper

Dynamical Stability of Bi-Directionally Graded Moving Beams

M.H. Babaei Rochi [1], J. Jamali [2,*]

[1] *Department of Mechanical Engineering, South Tehran Branch, Islamic Azad University, Tehran, Iran*
[2] *Department of Mechanical Engineering, Shoushtar Branch, Islamic Azad University, Shoushtar, Iran*

ABSTRACT

This article gravitates toward analyzing the vibration response of a moving beam functionally graded (FG) in two orthogonal directions. In order to gain a high level of accuracy, higher-order shear deformation theory for beam structures is employed to define the displacement field and determine the system's governing differential equations. Also, this study considers the effect of different sets of boundary conditions to find the oscillatory response of the system in a more comprehensive way. This matter leads the authors to utilize the differential quadrature method (DQM) as a numerical solution to solve the governing differential equations. The accuracy of the applied solution is examined and confirmed by comparing its results with those available in the literature. In this study, the natural frequency of a moving beam with varying properties along both the axial and transverse directions was investigated. The study examined the influence of boundary conditions, gradational properties, axial velocity, and the parameter L/h on the natural frequency. One of the applicable results for related industries is that designers should pay special attention to the FG power index, and the type of boundary conditions of the moving beams. This study provides novel insights to adjust design factors in order to gain a high level of vibration response for moving loads.

Keywords: Free vibration; Functionally graded axially moving beam; Instability; Differential quadrature method; Higher-order shear deformation theory.

1 INTRODUCTION

FUNCTIONALLY Graded Beams (FGBs) have gained significant attention in structural engineering due to their unique material properties and versatility in various applications [1]. FGBs exhibit spatial variation in

---

*Corresponding author. Tel.: +98 22983914.
E-mail address: jalil.jamali@iau.ac.ir
.

material composition, enabling tailored mechanical characteristics along the length and thickness of the beam [2]. FGBs find extensive applications in aerospace engineering [3]. The gradual variation of material properties in FGBs allows for enhanced performance in structural components such as wing spars [4], fuselage frames, and rotor blades [5]. FGBs can be designed to provide optimal strength-to-weight ratios [6], improved load-bearing capacity [7], and resistance to high-temperature gradients [8]. Additionally, FGBs offer excellent thermal stability, making them suitable for aerospace applications that involve extreme operating conditions [9]. In civil engineering, FGBs are utilized in various structural elements [10]. They are employed in bridge decks, beams, columns, and other load-bearing members [11]. FGBs can effectively withstand dynamic loads, vibrations, and thermal expansion/contraction [12]. The tailoring of material properties in FGBs allows for improved durability, reduced weight, and better resistance to corrosion, making them suitable for long-span structures and infrastructure exposed to harsh environments [13].

FGBs find applications in mechanical engineering, particularly in the design of rotating machinery components such as turbine blades [14], crankshafts [15], and camshafts [16]. By incorporating FGBs in these components, it is possible to optimize their performance and reliability [17]. The tailored material properties of FGBs enable the achievement of desired characteristics, such as improved strength [18], reduced stress concentrations [19], and enhanced fatigue resistance [20]. FGBs also offer the advantage of minimizing weight, contributing to overall energy efficiency [21]. FGBs have applications in energy systems, including wind turbines and solar panel structures [22,23]. In wind turbines, FGBs can be used to optimize the performance of blades, providing improved energy capture and reduced material usage [24]. Similarly, in solar panel structures, FGBs can enhance the structural integrity and efficiency of the components [25]. The ability to tailor material properties in FGBs allows for better utilization of renewable energy resources [26]. In biomedical engineering, FGBs are employed in the design and fabrication of various prosthetic devices and implants [27]. By tailoring the material composition along the length and thickness of the beam, FGBs can mimic the mechanical properties of natural tissues and bones [28]. This allows for improved biocompatibility and reduced stress shielding, leading to better integration with the human body [29]. FGBs have been utilized in dental implants [30], bone plates [31], and joint replacements [32], among other applications, to enhance patient outcomes and increase longevity.

Tabarrok et al. [33] gave an examination of the dynamic stability of a beam that moves axially. Kong et al. [34] investigated the approximate Eigen-solutions of axially moving beams with low flexural stiffness. Ref. [35] conducted a study on the non-linear vibrations and stability of a beam that moves axially at a velocity that varies over time. Beni et al. [36] conducted an investigation on the torsional behavior of flexoelectric micro/nanotubes made of porous functionally graded materials, taking into account the size dependency and the coupling between electromechanical effects. Beni et al. [37] conducted a study on the dynamic stability analysis of a nano-beam made of viscoelastic/piezoelectric material, taking into account its size dependence. Sze et al. [38] investigated the use of the incremental harmonic balance technique to analyze the nonlinear vibration of axially moving beams. Chen et al. [39] conducted a study on the use of the multidimensional Lindstedt-Poincaré technique to analyze the nonlinear vibration of axially moving beams. Ref. [40] conducted a study on the natural frequencies of nonlinear vibration in axially moving beams. Karimipour and colleagues [41] conducted a study on the nonlinear dynamic analysis of nonlocal composite laminated toroidal shell segments under mechanical stress.

Despite numerous analyses carried out to determine the mechanical response of the functionally graded structures, there is no record of exploring the vibration of bi-directionally graded moving beams among them. Accordingly, this article gravitates toward analyzing the vibration response of a moving beam functionally graded in two orthogonal directions. In order to gain a high level of accuracy, higher-order shear deformation theory for beam structures is employed to define the displacement field and determine the system's governing differential equations. Also, this study considers the effect of different sets of boundary conditions to find the oscillatory response of the system in a more comprehensive way. This matter leads the authors to utilize the differential quadrature method (DQM) as a numerical solution to solve the governing differential equations.

2   MATHEMATICAL MODELING

The schematic of the bi-directionally graded moving beams with their corresponding dimensions is shown in Fig. 1.
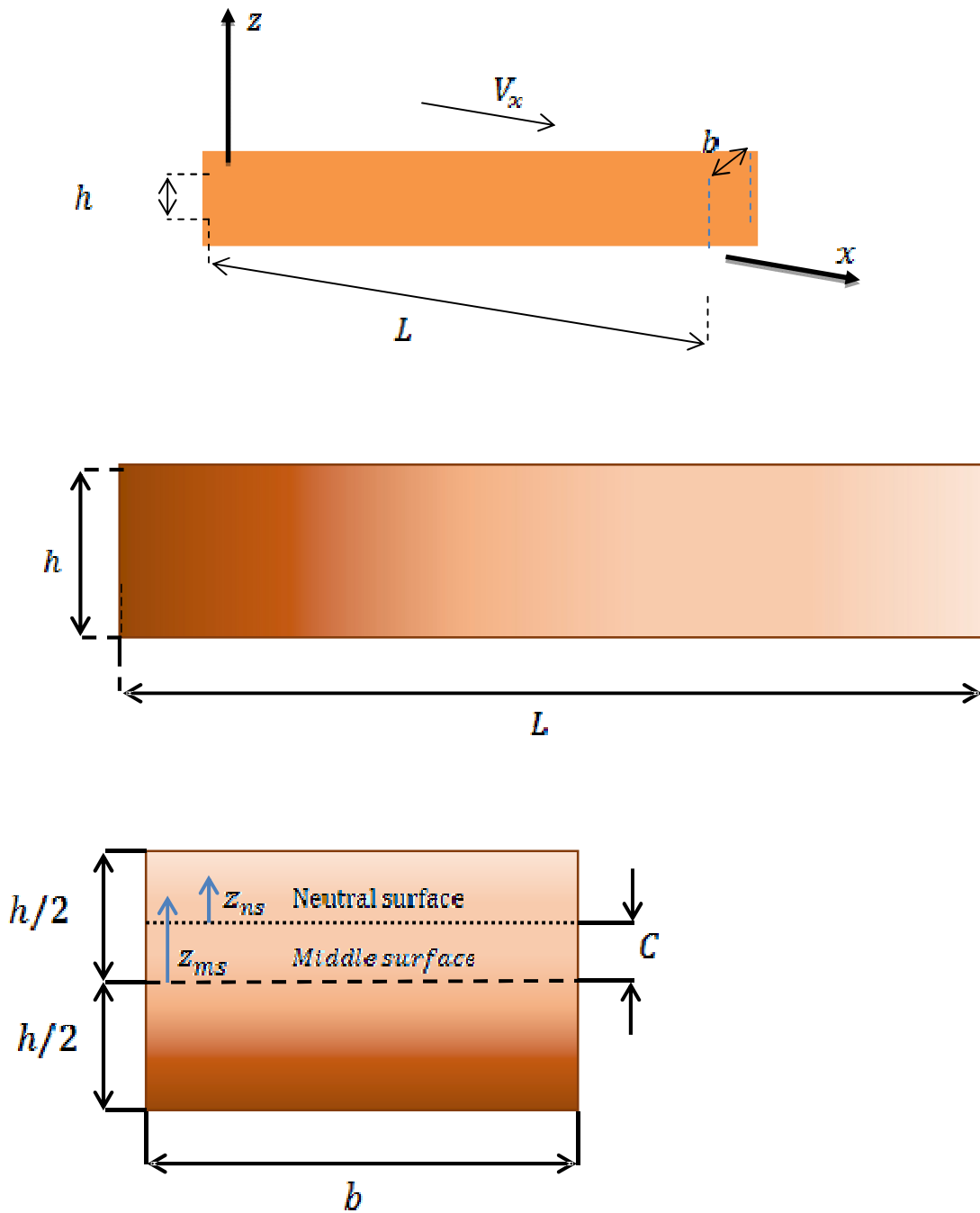
Fig. 1
Schematic of bi-directionally graded moving beams.

The circumstance of the neutral axis of the beam is intended to satisfy the first moment due to Young's modulus being zero as given below [42]

$$\int_{-h/2}^{h/2} E(z_{ms})(z_{ms} - C)dz_{ms} = 0,$$

(1)

Thus, the circumstance of the neutral surface can be given as

$$C = \frac{\int_{-h/2}^{h/2} E(z_{ms})z_{ms}dz_{ms}}{\int_{-h/2}^{h/2} E(z_{ms})dz_{ms}}.$$

(2)

Note: the neutral surface is zero for homogeneous beams, as expected.

Based on modified power law, material property P of the Bi-FGMs layer is defined as [43],

$$P(x, y, z) = P_m + (P_c - P_m)\left(\frac{x}{L}\right)^{n_x}\left(\frac{z_{ns} + C}{h} + 0.5\right)^{n_z},$$

(3)

In Eq. (3), P_c, and P_m are the material properties of the structure in $x=0$, $z=-h/2$, and $x=L$, $z=h/2$, respectively. It should be noted that n_x, and n_z show the FG power index along with axial, and transverse directions, respectively.

The materials properties of bi-directionally graded layer are as follows:

Table 1

Material characteristics of the bi-directionally graded moving beams [44].

Source	Symbol	Definition	Value	Unit
Ceramic (Silicon Nitride)	ϑ_c	Poisson's ratio of ceramic	0.24	—
	ρ_c	Mass density of ceramic	2370	$\frac{kg}{m^3}$
	E_c	Elastic modulus of ceramic	348.43×10^9	Pa
Metal (Stainless Steel)	ϑ_m	Poisson's ratio of metal	0.3262	—
	ρ_m	Mass density of metal	8166	$\frac{kg}{m^3}$
	E_m	Elastic modulus of metal	201.4×10^9	Pa

Consider an Bi-FG beam with length L and rectangular cross-section $b \times h$, with b being the width and h being the height. The beam is made of isotropic material with material properties varying smoothly in the thickness direction. The assumptions of the present theory are as follows:

1) The origin of the Cartesian coordinate system is taken at the neutral surface of the Bi-FG beam.
2) The effect of temperature and moisture is ignored.
3) The displacements are small in comparison with the height of the beam and, therefore, strains involved are infinitesimal

Based on the above assumptions, we have [45]:

$$u(x, z, t) = u_0(x, t) + zu_1(x, t) + z^2u_2(x, t) + z^3u_3(x, t),$$
$$v(x, z, t) = 0,$$
$$w(x, y, z, t) = w_0(x, t) + zw_1(x, t) + z^2w_2(x, t) + z^3w_3(x, t).$$

(4)

The strain–stress equations of the structure can be given as follows [45]:

$$\begin{Bmatrix} \sigma_x \\ \sigma_z \\ \tau_{xz} \end{Bmatrix} = \begin{bmatrix} Q_{11} & Q_{13} & 0 \\ Q_{13} & Q_{33} & 0 \\ 0 & 0 & Q_{55} \end{bmatrix} \begin{Bmatrix} \varepsilon_x \\ \varepsilon_z \\ \gamma_{xz} \end{Bmatrix},$$

(5)

where

$$Q_{11} = Q_{33} = \frac{E(x,z)}{\left(1-(\vartheta(x,z))^2\right)}, \quad Q_{13} = \frac{E(x,z)\vartheta(x,z)}{\left(1-(\vartheta(x,z))^2\right)}, \quad Q_{55} = \frac{E(x,z)}{2(1+\vartheta(x,z))}.$$

(6)

where $(\sigma_{xx}, \sigma_{zz}, \tau_{xz})$ are the stresses and $(\varepsilon_{xx}, \varepsilon_{zz}, \gamma_{xz})$ shows the linear strain and the Q_{ij}'s are elastic constants with reference to the *x-z* axes.

For obtaining the equations of motions along with associated end conditions of the bi-directionally graded moving beams, We can use from variational energy method as follows [46–50]:

$$\int_{t_1}^{t_2} (\delta T - \delta U) dt = 0,$$

(7)

In which kinetic energy of the system is [50]:

$$T = \int_V \frac{1}{2} \rho(x,z) \left[\left(V_x + \frac{D}{Dt}u\right)^2 + \left(\frac{D}{Dt}w\right)^2 \right] dV$$

(8)

where

$$\frac{D}{Dt} = \frac{\partial}{\partial t} + V_x \frac{\partial}{\partial x},$$
$$\frac{D^2}{Dt^2} = \frac{\partial^2}{\partial t^2} + 2V_x \frac{\partial^2}{\partial x \partial t} + V_x^2 \frac{\partial^2}{\partial x^2}.$$

(9)

Also, the strain energy of these bi-directionally graded moving beams can be attained through the following equation [51].

$$U = \iiint_V \sigma_{ij} \varepsilon_{ij} dV = \int_{-\square/2-c}^{\square/2-c} \iint_A \left(\sigma_{xx} \varepsilon_{xx} + \sigma_{zz} \delta \varepsilon_{zz} + \tau_{yz} \gamma_{yz} \right) dA dz.$$

(10)

Finally, by using Eqs. (8), (9), and (10) in Eq. (7), the motion equations of the bi-directionally graded moving beams are acquired as:

$$\delta u_0 : \quad \begin{aligned} & \frac{\partial N_{xx}}{\partial x} = \left(I_0 \frac{\partial^2 u_0}{\partial t^2} + I_1 \frac{\partial^2 u_1}{\partial t^2} + I_2 \frac{\partial^2 u_2}{\partial t^2} + I_3 \frac{\partial^2 u_3}{\partial t^2} \right) \\ & +2V_x \frac{\partial^2}{\partial x \partial t} (I_0 u_0 + I_1 u_1 + I_2 u_2 + I_3 u_3) \\ & +V_x^2 \frac{\partial^2}{\partial x^2} (I_0 u_0 + I_1 u_1 + I_2 u_2 + I_3 u_3), \end{aligned}$$

$$\delta w_0 : \quad \begin{aligned} & \frac{\partial N_{xz}}{\partial x} = \left(I_0 \frac{\partial^2 w_0}{\partial t^2} + I_1 \frac{\partial^2 w_1}{\partial t^2} + I_2 \frac{\partial^2 w_2}{\partial t^2} + I_3 \frac{\partial^2 w_3}{\partial t^2} \right) \\ & +2V_x \frac{\partial^2}{\partial x \partial t} (I_0 w_0 + I_1 w_1 + I_2 w_2 + I_3 w_3) \\ & +V_x^2 \frac{\partial^2}{\partial x^2} (I_0 w_0 + I_1 w_1 + I_2 w_2 + I_3 w_3), \end{aligned}$$

$$\delta u_1 : \quad \begin{aligned} & \frac{\partial M_{xx}}{\partial x} - N_{xz} = \left(I_1 \frac{\partial^2 u_0}{\partial t^2} + I_2 \frac{\partial^2 u_1}{\partial t^2} + I_3 \frac{\partial^2 u_2}{\partial t^2} + I_4 \frac{\partial^2 u_3}{\partial t^2} \right) \\ & +2V_x \frac{\partial^2}{\partial x \partial t} (I_1 u_0 + I_2 u_1 + I_3 u_2 + I_4 u_3) \\ & +V_x^2 \frac{\partial^2}{\partial x^2} (I_1 u_0 + I_2 u_1 + I_3 u_2 + I_4 u_3), \end{aligned}$$

$$\delta w_1 : \quad \begin{aligned} & \frac{\partial M_{xz}}{\partial x} - N_{zz} = \left(I_1 \frac{\partial^2 w_0}{\partial t^2} + I_2 \frac{\partial^2 w_1}{\partial t^2} + I_3 \frac{\partial^2 w_2}{\partial t^2} + I_4 \frac{\partial^2 w_3}{\partial t^2} \right) \\ & +2V_x \frac{\partial^2}{\partial x \partial t} (I_1 w_0 + I_2 w_1 + I_3 w_2 + I_4 w_3) \\ & +V_x^2 \frac{\partial^2}{\partial x^2} (I_1 w_0 + I_2 w_1 + I_3 w_2 + I_4 w_3). \end{aligned}$$

(11)

$$\frac{\partial P_{xx}}{\partial x} - 2M_{xz} = \left(I_2 \frac{\partial^2 u_0}{\partial t^2} + I_3 \frac{\partial^2 u_1}{\partial t^2} + I_4 \frac{\partial^2 u_2}{\partial t^2} + I_5 \frac{\partial^2 u_3}{\partial t^2} \right)$$

$$\delta u_2 \quad : \quad + 2V_x \frac{\partial^2}{\partial x \partial t} (I_2 u_0 + I_3 u_1 + I_4 u_2 + I_5 u_3) \qquad ,$$

$$+ V_x^2 \frac{\partial^2}{\partial x^2} (I_2 u_0 + I_3 u_1 + I_4 u_2 + I_5 u_3),$$

$$\frac{\partial P_{xz}}{\partial x} - 2M_{zz} = \left(I_2 \frac{\partial^2 w_0}{\partial t^2} + I_3 \frac{\partial^2 w_1}{\partial t^2} + I_4 \frac{\partial^2 w_2}{\partial t^2} + I_5 \frac{\partial^2 w_3}{\partial t^2} \right)$$

$$\delta w_2 \quad : \quad + 2V_x \frac{\partial^2}{\partial x \partial t} (I_2 w_0 + I_3 w_1 + I_4 w_2 + I_5 w_3) \qquad ,$$

$$+ V_x^2 \frac{\partial^2}{\partial x^2} (I_2 w_0 + I_3 w_1 + I_4 w_2 + I_5 w_3),$$

$$\frac{\partial Q_{xx}}{\partial x} - 3P_{xz} = \left(I_3 \frac{\partial^2 u_0}{\partial t^2} + I_4 \frac{\partial^2 u_1}{\partial t^2} + I_5 \frac{\partial^2 u_2}{\partial t^2} + I_6 \frac{\partial^2 u_3}{\partial t^2} \right)$$

$$\delta u_3 \quad : \quad + 2V_x \frac{\partial^2}{\partial x \partial t} (I_3 u_0 + I_4 u_1 + I_5 u_2 + I_6 u_3) \qquad ,$$

$$+ V_x^2 \frac{\partial^2}{\partial x^2} (I_3 u_0 + I_4 u_1 + I_5 u_2 + I_6 u_3),$$

$$\frac{\partial Q_{xz}}{\partial x} - 3P_{zz} = \left(I_3 \frac{\partial^2 w_0}{\partial t^2} + I_4 \frac{\partial^2 w_1}{\partial t^2} + I_5 \frac{\partial^2 w_2}{\partial t^2} + I_6 \frac{\partial^2 w_3}{\partial t^2} \right)$$

$$\delta w_3 \quad : \quad + 2V_x \frac{\partial^2}{\partial x \partial t} (I_3 w_0 + I_4 w_1 + I_5 w_2 + I_6 w_3) \qquad .$$

$$+ V_x^2 \frac{\partial^2}{\partial x^2} (I_3 w_0 + I_4 w_1 + I_5 w_2 + I_6 w_3),$$

In which:

$$\{N_{ii}, M_{ii}, P_{ii}, Q_{ii}\} = \int_0^L \int_{-\frac{h}{2}-c}^{\frac{h}{2}-c} \sigma_{ii} \{1, z, z^2, z^3\} dz dx \, ; \, i = x, z,$$

$$\{N_{ij}, M_{ij}, P_{ij}, Q_{ij}\} = \int_0^L \int_{-\frac{h}{2}-c}^{\frac{h}{2}-c} \tau_{ij} \{1, z, z^2, z^3\} dz dx \, ; \, i, j = x, z,$$

$$\{I_0, I_1, I_2, I_3, I_4, I_5, I_6\} = \int_0^L \int_{-\frac{h}{2}-c}^{\frac{h}{2}-c} \rho(x, z) \{1, z, z^2, z^3, z^4, z^5, z^6\} dz dx.$$

(12)

Also, the boundary conditions of the current system are:

$$\delta u_0 \quad : \quad N_{xx} \hat{n}_x = 0, \qquad\qquad \delta w_0 \quad : \quad N_{xz} \hat{n}_x = 0,$$

$$\delta u_1 \quad : \quad M_{xx} \hat{n}_x = 0, \qquad\qquad \delta w_1 \quad : \quad M_{xz} \hat{n}_x = 0,$$

$$\delta u_2 \quad : \quad P_{xx} \hat{n}_x = 0, \qquad\qquad \delta w_2 \quad : \quad P_{xz} \hat{n}_x = 0,$$

$$\delta u_3 \quad : \quad Q_{xx} \hat{n}_x = 0, \qquad\qquad \delta w_3 \quad : \quad Q_{xz} \hat{n}_x = 0,$$

(13)

3   NUMERICAL SOLUTION

This section outlines the key steps involved in achieving a numerical solution using the DQM.

3.1. Differential quadrature method (DQM)

Based on the principles of DQM, the *p*th derivative of $\mathcal{F}(x)$ as a one-dimensional function can be acquired as [51]

$$\frac{\partial^p \mathcal{F}(x)}{\partial x^p} = \sum_{j=1}^{N_x} \mathcal{A}_{ij}^{(p)} \mathcal{F}(x) \ for \ i = 1,2,\ldots,N_x \ and \ p = 1,2,\ldots,N_x - 1.$$

(14)

here $\mathcal{A}_{ij}^{(p)}$ signifies the weight coefficients for the ith grid-point $(j = 1,2,\ldots,N_x)$ and N_x signifies the grid-points' total number.

According to Eq. (15), $\mathcal{A}_{ij}^{(p)}$ for $i \neq j$ can be achieved as

$$\mathcal{A}_{ij}^{(p)} = n\left(\mathcal{A}_{ii}^{(p-1)}\mathcal{A}_{ij}^{(1)} - \frac{\mathcal{A}_{ij}^{(p-1)}}{x_i - x_j}\right), p = 2,3,\ldots,N_x - 1 \ and \ i,j = 1,2,\ldots,N_x,$$

(15)

here $A_{ij}^{(1)}$ would be formulated by the next relation

$$\mathcal{A}_{ij}^{(1)} = \frac{\mathcal{M}^{(1)}(x_i)}{(x_i - x_j)\mathcal{M}^{(1)}(x_j)}, i,j = 1,2,\ldots,N_x,$$

(16)

Next relationship would be employed to acquire $\mathcal{A}_{ij}^{(p)}$

$$\mathcal{A}_{ii}^{(p)} = -\sum_{j=1,j\neq i}^{N} \mathcal{A}_{ij}^{(p)}, i = 2,3,\ldots,N_x \ and \ p = 1,2,\ldots,N_x - 1,$$

(17)

$\mathcal{M}^{(1)}$ in Eq. (16) can be derived as

$$\mathcal{M}^{(1)}(x_k) = -\sum_{j=1,j\neq k}^{N_x}(x_k - x_j), for \ k = 1,2,3,\ldots,N_x.$$

(18)

The grid-points (x_i) can be achieved as below, with the aid of the Chebyshev–Gauss–Lobatto function [51]

$$x_i = \frac{L}{2}\left(1 - \cos\left(\frac{(i-1)}{(N_x-1)}\pi\right)\right) i = 1,2,3,\ldots,N_x,$$

(19)

In addition to, the displacement field can be written as below,

$$u_i(x,t) = U_i(x)e^{i\omega t} \quad i = 0,1,2,3.$$

(20)

$$w_i(x,t) = W_i(x) e^{i\omega t} \quad i = 0,1,2,3.$$

By substituting Eqs. (12), (14), and (20) in to Eq. (11) we have:

$$\delta u_0: \left\{ A_{11} \sum_{p=1}^{N} g_{ip}^{(2)} U_{0pj} + B_{11} \sum_{p=1}^{N} g_{ip}^{(2)} U_{1pj} + C_{11} \sum_{p=1}^{N} g_{ip}^{(2)} U_{2pj} \right.$$

$$+ D_{11} \sum_{p=1}^{N} g_{ip}^{(2)} U_{3pj} + A_{13} \sum_{p=1}^{N} g_{ip}^{(1)} W_{0pj} + 2B_{13} \sum_{p=1}^{N} g_{ip}^{(1)} W_{1pj}$$

$$\left. + 3C_{13} \sum_{p=1}^{N} g_{ip}^{(1)} W_{3pj} \right\}$$

$$+ \left\{ A_{11}^{(1)} \sum_{p=1}^{N} g_{ip}^{(1)} U_{0pj} + B_{11}^{(1)} \sum_{p=1}^{N} g_{ip}^{(1)} U_{1pj} + C_{11}^{(1)} \sum_{p=1}^{N} g_{ip}^{(1)} U_{2pj} \right.$$

$$\left. + D_{11}^{(1)} \sum_{p=1}^{N} g_{ip}^{(1)} U_{3pj} + A_{13}^{(1)} \sum_{p=1}^{N} I_{ip} W_{0pj} + 2B_{13}^{(1)} \sum_{p=1}^{N} I_{ip} W_{2pj} + 3C_{13}^{(1)} \sum_{p=1}^{N} I_{ip} \right\}$$

$$= -\omega^2 \begin{pmatrix} I_0 U_{0ij} + I_1 U_{1ij} \\ + I_2 U_{2ij} + I_3 U_{3ij} \end{pmatrix} + 2V_x i\omega \begin{pmatrix} I_0 \sum_{p=1}^{N} g_{ip}^{(1)} U_{0pj} + I_1 \sum_{p=1}^{N} g_{ip}^{(1)} U_{1pj} \\ + I_2 \sum_{p=1}^{N} g_{ip}^{(1)} U_{2pj} + I_3 \sum_{p=1}^{N} g_{ip}^{(1)} U_{3pj} \end{pmatrix}$$

$$+ 2V_x i\omega \begin{pmatrix} \dfrac{\partial I_0}{\partial x} U_{0ij} + \dfrac{\partial I_1}{\partial x} U_{1ij} \\ + \dfrac{\partial I_2}{\partial x} U_{2ij} + \dfrac{\partial I_3}{\partial x} U_{3ij} \end{pmatrix} + V_x^2 \begin{pmatrix} I_0 \sum_{p=1}^{N} g_{ip}^{(2)} U_{0pj} + I_1 \sum_{p=1}^{N} g_{ip}^{(2)} U_{1pj} \\ + I_2 \sum_{p=1}^{N} g_{ip}^{(2)} U_{2pj} + I_3 \sum_{p=1}^{N} g_{ip}^{(2)} U_{3p} \end{pmatrix}$$

$$+ 2V_x^2 \begin{pmatrix} \dfrac{\partial I_0}{\partial x} \sum_{p=1}^{N} g_{ip}^{(1)} U_{0pj} + \dfrac{\partial I_1}{\partial x} \sum_{p=1}^{N} g_{ip}^{(1)} U_{1pj} \\ + \dfrac{\partial I_2}{\partial x} \sum_{p=1}^{N} g_{ip}^{(1)} U_{2pj} + \dfrac{\partial I_3}{\partial x} \sum_{p=1}^{N} g_{ip}^{(1)} U_{3pj} \end{pmatrix} + V_x^2 \begin{pmatrix} \dfrac{\partial^2 I_0}{\partial x^2} U_{0ij} + \dfrac{\partial^2 I_1}{\partial x^2} U_{1ij} \\ + \dfrac{\partial^2 I_2}{\partial x^2} U_{2ij} + \dfrac{\partial^2 I_3}{\partial x^2} U_{3ij} \end{pmatrix} \tag{21a}$$

$$\delta w_0 : \left\{ A_{55} \sum_{p=1}^{N} g_{ip}^{(1)} U_{1pj} + 2B_{55} \sum_{p=1}^{N} g_{ip}^{(1)} U_{2pj} + 3C_{55} \sum_{p=1}^{N} g_{ip}^{(1)} U_{3pj} + A_{55} \sum_{p=1}^{N} g_{ip}^{(2)} W_{0pj} \right.$$

$$\left. + B_{55} \sum_{p=1}^{N} g_{ip}^{(2)} W_{1pj} + C_{55} \sum_{p=1}^{N} g_{ip}^{(2)} W_{2pj} + D_{55} \sum_{p=1}^{N} g_{ip}^{(2)} W_{3pj} \right\}$$

$$+ \left\{ A_{55}^{(1)} \sum_{p=1}^{N} I_{ip} U_{1pj} + 2B_{55}^{(1)} \sum_{p=1}^{N} I_{ip} U_{2pj} + 3C_{55}^{(1)} \sum_{p=1}^{N} I_{ip} U_{3pj} + A_{55}^{(1)} \sum_{p=1}^{N} \right.$$

$$\left. + B_{55}^{(1)} \sum_{p=1}^{N} g_{ip}^{(1)} W_{1pj} + C_{55}^{(1)} \sum_{p=1}^{N} g_{ip}^{(1)} W_{2pj} + D_{55}^{(1)} \sum_{p=1}^{N} g_{ip}^{(1)} W_{3pj} \right\}$$

$$= -\omega^2 \left(\begin{matrix} I_0 W_{0ij} + I_1 W_{1ij} \\ + I_2 W_{2ij} + I_3 W_{3ij} \end{matrix} \right) + 2V_x l\omega \left(\begin{matrix} I_0 \sum_{p=1}^{N} g_{ip}^{(1)} W_{0pj} + I_1 \sum_{p=1}^{N} g_{ip}^{(1)} W \\ + I_2 \sum_{p=1}^{N} g_{ip}^{(1)} W_{2pj} + I_3 \sum_{p=1}^{N} g_{ip}^{(1)} \end{matrix} \right)$$

$$+ 2V_x l\omega \left(\begin{matrix} \dfrac{\partial I_0}{\partial x} W_{0ij} + \dfrac{\partial I_1}{\partial x} W_{1ij} \\ + \dfrac{\partial I_2}{\partial x} W_{2ij} + \dfrac{\partial I_3}{\partial x} W_{3ij} \end{matrix} \right) + V_x^2 \left(\begin{matrix} I_0 \sum_{p=1}^{N} g_{ip}^{(2)} W_{0pj} + I_1 \sum_{p=1}^{N} g_{ip}^{(2} \\ + I_2 \sum_{p=1}^{N} g_{ip}^{(2)} W_{2pj} + I_3 \sum_{p=1}^{N} g \end{matrix} \right)$$

$$+ 2V_x^2 \left(\begin{matrix} \dfrac{\partial I_0}{\partial x} \sum_{p=1}^{N} g_{ip}^{(1)} W_{0pj} + \dfrac{\partial I_1}{\partial x} \sum_{p=1}^{N} g_{ip}^{(1)} W_{1pj} \\ + \dfrac{\partial I_2}{\partial x} \sum_{p=1}^{N} g_{ip}^{(1)} W_{2pj} + \dfrac{\partial I_3}{\partial x} \sum_{p=1}^{N} g_{ip}^{(1)} W_{3pj} \end{matrix} \right) + V_x^2 \left(\begin{matrix} \dfrac{\partial^2 I_0}{\partial x^2} W_{0ij} + \dfrac{\partial^2 I_1}{\partial x^2} W_{1ij} \\ + \dfrac{\partial^2 I_2}{\partial x^2} W_{2ij} + \dfrac{\partial^2 I_3}{\partial x^2} W_{3ij} \end{matrix} \right) \tag{21b}$$

$$\delta u_1: \left\{ B_{11} \sum_{p=1}^{N} g_{ip}^{(2)} U_{0pj} + C_{11} \sum_{p=1}^{N} g_{ip}^{(2)} U_{1pj} + D_{11} \sum_{p=1}^{N} g_{ip}^{(2)} U_{2pj} + E_{11} \sum_{p=1}^{N} g_{ip}^{(2)} U_{3pj} \right.$$

$$\left. + B_{13} \sum_{p=1}^{N} g_{ip}^{(1)} W_{1pj} + 2C_{13} \sum_{p=1}^{N} g_{ip}^{(1)} W_{2pj} + 3D_{13} \sum_{p=1}^{N} g_{ip}^{(1)} W_{3pj} \right\}$$

$$+ \left\{ B_{11}^{(1)} \sum_{p=1}^{N} g_{ip}^{(1)} U_{0pj} + C_{11}^{(1)} \sum_{p=1}^{N} g_{ip}^{(1)} U_{1pj} + D_{11}^{(1)} \sum_{p=1}^{N} g_{ip}^{(1)} U_{2pj} \right.$$

$$+ E_{11}^{(1)} \sum_{p=1}^{N} g_{ip}^{(1)} U_{3pj} + B_{13}^{(1)} \sum_{p=1}^{N} I_{ip} W_{0pj} + 2C_{13}^{(1)} \sum_{p=1}^{N} I_{ip} W_{2pj} + 3D_{13}^{(1)} \sum_{p=}$$

$$- \left\{ A_{55} U_{1ij} + 2B_{55} U_{2ij} + 3C_{55} U_{3ij} + A_{55} \sum_{p=1}^{N} g_{ip}^{(1)} W_{0pj} + B_{55} \sum_{p=1}^{N} g_{ip}^{(1)} \right.$$

$$\left. + C_{55} \sum_{p=1}^{N} g_{ip}^{(1)} W_{2pj} + D_{55} \sum_{p=1}^{N} g_{ip}^{(1)} W_{3pj} \right\}$$

$$= -\omega^2 \begin{pmatrix} I_1 U_{0ij} + I_2 U_{1ij} \\ + I_3 U_{2ij} + I_4 U_{3ij} \end{pmatrix} + 2V_x i\omega \left(I_1 \sum_{p=1}^{N} g_{ip}^{(1)} U_{0pj} + I_2 \sum_{p=1}^{N} g_{ip}^{(1)} U_{1p} \right.$$

$$\left. + I_3 \sum_{p=1}^{N} g_{ip}^{(1)} U_{2pj} + I_4 \sum_{p=1}^{N} g_{ip}^{(1)} U \right.$$

$$+ 2V_x i\omega \begin{pmatrix} \dfrac{\partial I_1}{\partial x} U_{0ij} + \dfrac{\partial I_2}{\partial x} U_{1ij} \\ + \dfrac{\partial I_3}{\partial x} U_{2ij} + \dfrac{\partial I_4}{\partial x} U_{3ij} \end{pmatrix} + V_x^2 \left(I_1 \sum_{p=1}^{N} g_{ip}^{(2)} U_{0pj} + I_2 \sum_{p=1}^{N} g_{ip}^{(2)} \right.$$

$$\left. + I_3 \sum_{p=1}^{N} g_{ip}^{(2)} U_{2pj} + I_4 \sum_{p=1}^{N} g_{ip}^{(} \right.$$

$$+ 2V_x^2 \begin{pmatrix} \dfrac{\partial I_1}{\partial x} \sum_{p=1}^{N} g_{ip}^{(1)} U_{0pj} + \dfrac{\partial I_2}{\partial x} \sum_{p=1}^{N} g_{ip}^{(1)} U_{1pj} \\ + \dfrac{\partial I_3}{\partial x} \sum_{p=1}^{N} g_{ip}^{(1)} U_{2pj} + \dfrac{\partial I_4}{\partial x} \sum_{p=1}^{N} g_{ip}^{(1)} U_{3pj} \end{pmatrix} + V_x^2 \begin{pmatrix} \dfrac{\partial^2 I_1}{\partial x^2} U_{0ij} + \dfrac{\partial^2 I_2}{\partial x^2} U_{1ij} \\ + \dfrac{\partial^2 I_3}{\partial x^2} U_{2ij} + \dfrac{\partial^2 I_4}{\partial x^2} U_{3ij} \end{pmatrix},$$

$$\tag{21c}$$

$$\delta w_1 : \left\{ B_{55} \sum_{p=1}^{N} g_{ip}^{(1)} U_{1pj} + 2C_{55} \sum_{p=1}^{N} g_{ip}^{(1)} U_{2pj} + 3D_{55} \sum_{p=1}^{N} g_{ip}^{(1)} U_{3pj} + B_{55} \sum_{p=1}^{N} g_{ip}^{(2)} W_{0pj} \right.$$

$$\left. + C_{55} \sum_{p=1}^{N} g_{ip}^{(2)} W_{1pj} + D_{55} \sum_{p=1}^{N} g_{ip}^{(2)} W_{2pj} + E_{55} \sum_{p=1}^{N} g_{ip}^{(2)} W_{3pj} \right\}$$

$$+ \left\{ B_{55}^{(1)} \sum_{p=1}^{N} I_{ip} U_{1pj} + 2C_{55}^{(1)} \sum_{p=1}^{N} I_{ip} U_{2pj} + 3D_{55}^{(1)} \sum_{p=1}^{N} I_{ip} U_{3pj} + B_{55}^{(1)} \sum_{p=1}^{N} \right.$$

$$\left. + C_{55}^{(1)} \sum_{p=1}^{N} g_{ip}^{(1)} W_{1pj} + D_{55}^{(1)} \sum_{p=1}^{N} g_{ip}^{(1)} W_{2pj} + E_{55}^{(1)} \sum_{p=1}^{N} g_{ip}^{(1)} W_{3pj} \right\}$$

$$- \left\{ A_{13} \sum_{p=1}^{N} g_{ip}^{(1)} U_{0pj} + B_{13} \sum_{p=1}^{N} g_{ip}^{(1)} U_{1pj} + C_{13} \sum_{p=1}^{N} g_{ip}^{(1)} U_{2pj} + D_{13} \sum_{p=1}^{N} \right.$$

$$\left. + A_{33} W_{1ij} + 2B_{33} W_{2ij} + 3C_{33} W_{3ij} \right\}$$

$$= -\omega^2 \left(\begin{array}{c} I_1 W_{0ij} + I_2 W_{1ij} \\ + I_3 W_{2ij} + I_4 W_{3ij} \end{array} \right) + 2V_x i\omega \left(\begin{array}{c} I_1 \sum_{p=1}^{N} g_{ip}^{(1)} W_{0pj} + I_2 \sum_{p=1}^{N} g_{ip}^{(1)} W \\ + I_3 \sum_{p=1}^{N} g_{ip}^{(1)} W_{2pj} + I_4 \sum_{p=1}^{N} g_{ip}^{(1)} \end{array} \right.$$

$$+ 2V_x i\omega \left(\begin{array}{c} \dfrac{\partial I_1}{\partial x} W_{0ij} + \dfrac{\partial I_2}{\partial x} W_{1ij} \\ + \dfrac{\partial I_3}{\partial x} W_{2ij} + \dfrac{\partial I_4}{\partial x} W_{3ij} \end{array} \right) + V_x^2 \left(\begin{array}{c} I_1 \sum_{p=1}^{N} g_{ip}^{(2)} W_{0pj} + I_2 \sum_{p=1}^{N} g_{ip}^{(2)} \\ + I_3 \sum_{p=1}^{N} g_{ip}^{(2)} W_{2pj} + I_4 \sum_{p=1}^{N} g \end{array} \right.$$

$$+ 2V_x^2 \left(\begin{array}{c} \dfrac{\partial I_1}{\partial x} \sum_{p=1}^{N} g_{ip}^{(1)} W_{0pj} + \dfrac{\partial I_2}{\partial x} \sum_{p=1}^{N} g_{ip}^{(1)} W_{1pj} \\ + \dfrac{\partial I_3}{\partial x} \sum_{p=1}^{N} g_{ip}^{(1)} W_{2pj} + \dfrac{\partial I_4}{\partial x} \sum_{p=1}^{N} g_{ip}^{(1)} W_{3pj} \end{array} \right) + V_x^2 \left(\begin{array}{c} \dfrac{\partial^2 I_1}{\partial x^2} W_{0ij} + \dfrac{\partial^2 I_2}{\partial x^2} W_{1ij} \\ + \dfrac{\partial^2 I_3}{\partial x^2} W_{2ij} + \dfrac{\partial^2 I_4}{\partial x^2} W_{3ij} \end{array} \right) \tag{19c}$$

$$\delta u_2: \left\{ C_{11} \sum_{p=1}^{N} g_{ip}^{(2)} U_{0pj} + D_{11} \sum_{p=1}^{N} g_{ip}^{(2)} U_{1pj} + E_{11} \sum_{p=1}^{N} g_{ip}^{(2)} U_{2pj} + F_{11} \sum_{p=1}^{N} g_{ip}^{(2)} U_{3pj} \right.$$

$$\left. + C_{13} \sum_{p=1}^{N} g_{ip}^{(1)} W_{1pj} + 2D_{13} \sum_{p=1}^{N} g_{ip}^{(1)} W_{2pj} + 3E_{13} \sum_{p=1}^{N} g_{ip}^{(1)} W_{3pj} \right\}$$

$$+ \left\{ C_{11}^{(1)} \sum_{p=1}^{N} g_{ip}^{(1)} U_{0pj} + D_{11}^{(1)} \sum_{p=1}^{N} g_{ip}^{(1)} U_{1pj} + E_{11}^{(1)} \sum_{p=1}^{N} g_{ip}^{(1)} U_{2pj} \right.$$

$$+ F_{11}^{(1)} \sum_{p=1}^{N} g_{ip}^{(1)} U_{3pj} + C_{13}^{(1)} \sum_{p=1}^{N} I_{ip} W_{0pj} + 2D_{13}^{(1)} \sum_{p=1}^{N} I_{ip} W_{2pj} + 3E_{13}^{(1)} \sum_{p=}$$

$$- 2 \left\{ B_{55} U_{1ij} + 2C_{55} U_{2ij} + 3D_{55} U_{3ij} + B_{55} \sum_{p=1}^{N} g_{ip}^{(1)} W_{0pj} + C_{55} \sum_{p=1}^{N} g_i \right.$$

$$\left. + D_{55} \sum_{p=1}^{N} g_{ip}^{(1)} W_{2pj} + E_{55} \sum_{p=1}^{N} g_{ip}^{(1)} W_{3pj} \right\}$$

$$= -\omega^2 \begin{pmatrix} I_2 U_{0ij} + I_3 U_{1ij} \\ + I_4 U_{2ij} + I_5 U_{3ij} \end{pmatrix} + 2V_x i\omega \begin{pmatrix} I_2 \sum_{p=1}^{N} g_{ip}^{(1)} U_{0pj} + I_3 \sum_{p=1}^{N} g_{ip}^{(1)} U_{1p} \\ + I_4 \sum_{p=1}^{N} g_{ip}^{(1)} U_{2pj} + I_5 \sum_{p=1}^{N} g_{ip}^{(1)} U \end{pmatrix}$$

$$+ 2V_x i\omega \begin{pmatrix} \frac{\partial I_2}{\partial x} U_{0ij} + \frac{\partial I_3}{\partial x} U_{1ij} \\ + \frac{\partial I_4}{\partial x} U_{2ij} + \frac{\partial I_5}{\partial x} U_{3ij} \end{pmatrix} + V_x^2 \begin{pmatrix} I_2 \sum_{p=1}^{N} g_{ip}^{(2)} U_{0pj} + I_3 \sum_{p=1}^{N} g_{ip}^{(2)} \\ + I_4 \sum_{p=1}^{N} g_{ip}^{(2)} U_{2pj} + I_5 \sum_{p=1}^{N} g_{i} \end{pmatrix}$$

$$+ 2V_x^2 \begin{pmatrix} \frac{\partial I_2}{\partial x} \sum_{p=1}^{N} g_{ip}^{(1)} U_{0pj} + \frac{\partial I_3}{\partial x} \sum_{p=1}^{N} g_{ip}^{(1)} U_{1pj} \\ + \frac{\partial I_4}{\partial x} \sum_{p=1}^{N} g_{ip}^{(1)} U_{2pj} + \frac{\partial I_5}{\partial x} \sum_{p=1}^{N} g_{ip}^{(1)} U_{3pj} \end{pmatrix} + V_x^2 \begin{pmatrix} \frac{\partial^2 I_2}{\partial x^2} U_{0ij} + \frac{\partial^2 I_3}{\partial x^2} U_{1ij} \\ + \frac{\partial^2 I_4}{\partial x^2} U_{2ij} + \frac{\partial^2 I_5}{\partial x^2} U_{3ij} \end{pmatrix},$$

(19d)

$$\delta w_2 : \left\{ C_{55} \sum_{p=1}^{N} g_{ip}^{(1)} U_{1pj} + 2D_{55} \sum_{p=1}^{N} g_{ip}^{(1)} U_{2pj} + 3E_{55} \sum_{p=1}^{N} g_{ip}^{(1)} U_{3pj} + C_{55} \sum_{p=1}^{N} g_{ip}^{(2)} W_{0pj} \right.$$

$$\left. + D_{55} \sum_{p=1}^{N} g_{ip}^{(2)} W_{1pj} + E_{55} \sum_{p=1}^{N} g_{ip}^{(2)} W_{2pj} + F_{55} \sum_{p=1}^{N} g_{ip}^{(2)} W_{3pj} \right\}$$

$$+ \left\{ C_{55}^{(1)} \sum_{p=1}^{N} I_{ip} U_{1pj} + 2D_{55}^{(1)} \sum_{p=1}^{N} I_{ip} U_{2pj} + 3E_{55}^{(1)} \sum_{p=1}^{N} I_{ip} U_{3pj} + C_{55}^{(1)} \sum_{p=1}^{N} \right.$$

$$\left. + D_{55}^{(1)} \sum_{p=1}^{N} g_{ip}^{(1)} W_{1pj} + E_{55}^{(1)} \sum_{p=1}^{N} g_{ip}^{(1)} W_{2pj} + F_{55}^{(1)} \sum_{p=1}^{N} g_{ip}^{(1)} W_{3pj} \right\}$$

$$- 2 \left\{ B_{13} \sum_{p=1}^{N} g_{ip}^{(1)} U_{0pj} + C_{13} \sum_{p=1}^{N} g_{ip}^{(1)} U_{1pj} + D_{13} \sum_{p=1}^{N} g_{ip}^{(1)} U_{2pj} + E_{13} \sum_{p=1}^{N} \right.$$

$$\left. + B_{33} W_{1ij} + 2C_{33} W_{2ij} + 3D_{33} W_{3ij} \right\}$$

$$= -\omega^2 \begin{pmatrix} I_2 W_{0ij} + I_3 W_{1ij} \\ + I_4 W_{2ij} + I_5 W_{3ij} \end{pmatrix} + 2V_x i\omega \left(I_2 \sum_{p=1}^{N} g_{ip}^{(1)} W_{0pj} + I_3 \sum_{p=1}^{N} g_{ip}^{(1)} W \right.$$

$$\left. + I_4 \sum_{p=1}^{N} g_{ip}^{(1)} W_{2pj} + I_5 \sum_{p=1}^{N} g_{ip}^{(1)} \right.$$

$$+ 2V_x i\omega \begin{pmatrix} \dfrac{\partial I_2}{\partial x} W_{0ij} + \dfrac{\partial I_3}{\partial x} W_{1ij} \\ + \dfrac{\partial I_4}{\partial x} W_{2ij} + \dfrac{\partial I_5}{\partial x} W_{3ij} \end{pmatrix} + V_x^2 \left(I_2 \sum_{p=1}^{N} g_{ip}^{(2)} W_{0pj} + I_3 \sum_{p=1}^{N} g_{ip}^{(2)} \right.$$

$$\left. + I_4 \sum_{p=1}^{N} g_{ip}^{(2)} W_{2pj} + I_5 \sum_{p=1}^{N} g \right.$$

$$+ 2V_x^2 \begin{pmatrix} \dfrac{\partial I_2}{\partial x} \sum_{p=1}^{N} g_{ip}^{(1)} W_{0pj} + \dfrac{\partial I_3}{\partial x} \sum_{p=1}^{N} g_{ip}^{(1)} W_{1pj} \\ + \dfrac{\partial I_4}{\partial x} \sum_{p=1}^{N} g_{ip}^{(1)} W_{2pj} + \dfrac{\partial I_5}{\partial x} \sum_{p=1}^{N} g_{ip}^{(1)} W_{3pj} \end{pmatrix} + V_x^2 \begin{pmatrix} \dfrac{\partial^2 I_2}{\partial x^2} W_{0ij} + \dfrac{\partial^2 I_3}{\partial x^2} W_{1ij} \\ + \dfrac{\partial^2 I_4}{\partial x^2} W_{2ij} + \dfrac{\partial^2 I_5}{\partial x^2} W_{3ij} \end{pmatrix}$$

$$(19f)$$

$$\delta u_3 : \left\{ D_{11} \sum_{p=1}^{N} g_{ip}^{(2)} U_{0pj} + E_{11} \sum_{p=1}^{N} g_{ip}^{(2)} U_{1pj} + F_{11} \sum_{p=1}^{N} g_{ip}^{(2)} U_{2pj} + G_{11} \sum_{p=1}^{N} g_{ip}^{(2)} U_{3pj} \right.$$

$$\left. + D_{13} \sum_{p=1}^{N} g_{ip}^{(1)} W_{1pj} + 2E_{13} \sum_{p=1}^{N} g_{ip}^{(1)} W_{2pj} + 3F_{13} \sum_{p=1}^{N} g_{ip}^{(1)} W_{3pj} \right\}$$

$$+ \left\{ D_{11}^{(1)} \sum_{p=1}^{N} g_{ip}^{(1)} U_{0pj} + E_{11}^{(1)} \sum_{p=1}^{N} g_{ip}^{(1)} U_{1pj} + F_{11}^{(1)} \sum_{p=1}^{N} g_{ip}^{(1)} U_{2pj} \right.$$

$$+ G_{11}^{(1)} \sum_{p=1}^{N} g_{ip}^{(1)} U_{3pj} + D_{13}^{(1)} \sum_{p=1}^{N} I_{ip} W_{0pj} + 2E_{13}^{(1)} \sum_{p=1}^{N} I_{ip} W_{2pj} + 3F_{13}^{(1)} \sum_{p=}$$

$$- 3 \left\{ C_{55} U_{1ij} + 2D_{55} U_{2ij} + 3E_{55} U_{3ij} + C_{55} \sum_{p=1}^{N} g_{ip}^{(1)} W_{0pj} + D_{55} \sum_{p=1}^{N} g \right.$$

$$\left. + E_{55} \sum_{p=1}^{N} g_{ip}^{(1)} W_{2pj} + F_{55} \sum_{p=1}^{N} g_{ip}^{(1)} W_{3pj} \right\}$$

$$= -\omega^2 \begin{pmatrix} I_3 U_{0ij} + I_4 U_{1ij} \\ + I_5 U_{2ij} + I_6 U_{3ij} \end{pmatrix} + 2V_x i\omega \left(I_3 \sum_{p=1}^{N} g_{ip}^{(1)} U_{0pj} + I_4 \sum_{p=1}^{N} g_{ip}^{(1)} U_{1?} \right.$$

$$\left. + I_5 \sum_{p=1}^{N} g_{ip}^{(1)} U_{2pj} + I_6 \sum_{p=1}^{N} g_{ip}^{(1)} U \right.$$

$$+ 2V_x i\omega \begin{pmatrix} \dfrac{\partial I_3}{\partial x} U_{0ij} + \dfrac{\partial I_4}{\partial x} U_{1ij} \\ + \dfrac{\partial I_5}{\partial x} U_{2ij} + \dfrac{\partial I_6}{\partial x} U_{3ij} \end{pmatrix} + V_x^2 \left(I_3 \sum_{p=1}^{N} g_{ip}^{(2)} U_{0pj} + I_4 \sum_{p=1}^{N} g_{ip}^{(2)} \right.$$

$$\left. + I_5 \sum_{p=1}^{N} g_{ip}^{(2)} U_{2pj} + I_6 \sum_{p=1}^{N} g_i^{(} \right.$$

$$+ 2V_x^2 \begin{pmatrix} \dfrac{\partial I_3}{\partial x} \sum_{p=1}^{N} g_{ip}^{(1)} U_{0pj} + \dfrac{\partial I_4}{\partial x} \sum_{p=1}^{N} g_{ip}^{(1)} U_{1pj} \\ + \dfrac{\partial I_5}{\partial x} \sum_{p=1}^{N} g_{ip}^{(1)} U_{2pj} + \dfrac{\partial I_6}{\partial x} \sum_{p=1}^{N} g_{ip}^{(1)} U_{3pj} \end{pmatrix} + V_x^2 \begin{pmatrix} \dfrac{\partial^2 I_3}{\partial x^2} U_{0ij} + \dfrac{\partial^2 I_4}{\partial x^2} U_{1ij} \\ + \dfrac{\partial^2 I_5}{\partial x^2} U_{2ij} + \dfrac{\partial^2 I_6}{\partial x^2} U_{3ij} \end{pmatrix}$$

(19g)

$$\delta w_3 : \left\{ D_{55} \sum_{p=1}^{N} g_{ip}^{(1)} U_{1pj} + 2E_{55} \sum_{p=1}^{N} g_{ip}^{(1)} U_{2pj} + 3F_{55} \sum_{p=1}^{N} g_{ip}^{(1)} U_{3pj} + D_{55} \sum_{p=1}^{N} g_{ip}^{(1)} W_{0pj} \right.$$

$$\left. + E_{55} \sum_{p=1}^{N} g_{ip}^{(1)} W_{1pj} + F_{55} \sum_{p=1}^{N} g_{ip}^{(1)} W_{2pj} + G_{55} \sum_{p=1}^{N} g_{ip}^{(1)} W_{3pj} \right\}$$

$$+ \left\{ D_{55}^{(1)} \sum_{p=1}^{N} I_{ip} U_{1pj} + 2E_{55}^{(1)} \sum_{p=1}^{N} I_{ip} U_{2pj} + 3F_{55}^{(1)} \sum_{p=1}^{N} I_{ip} U_{3pj} \right.$$

$$\left. + D_{55}^{(1)} \sum_{p=1}^{N} g_{ip}^{(1)} W_{0pj} \right\}$$

$$- 3 \left\{ C_{13} \sum_{p=1}^{N} g_{ip}^{(1)} U_{0pj} + D_{13} \sum_{p=1}^{N} g_{ip}^{(1)} U_{1pj} + E_{13} \sum_{p=1}^{N} g_{ip}^{(1)} U_{2pj} + F_{13} \sum_{p=} \right.$$

$$\left. + C_{33} W_{1ij} + 2D_{33} W_{2ij} + 3E_{33} W_{3ij} \right\}$$

$$= -\omega^2 \binom{I_3 W_{0ij} + I_4 W_{1ij}}{+ I_5 W_{2ij} + I_6 W_{3ij}} + 2V_x i\omega \left(I_3 \sum_{p=1}^{N} g_{ip}^{(1)} W_{0pj} + I_4 \sum_{p=1}^{N} g_{ip}^{(1)} W \right.$$

$$\left. + I_5 \sum_{p=1}^{N} g_{ip}^{(1)} W_{2pj} + I_6 \sum_{p=1}^{N} g_{ip}^{(1)} \right.$$

$$+ 2V_x i\omega \left(\frac{\partial I_3}{\partial x} W_{0ij} + \frac{\partial I_4}{\partial x} W_{1ij} \right) + V_x^2 \left(I_3 \sum_{p=1}^{N} g_{ip}^{(2)} W_{0pj} + I_4 \sum_{p=1}^{N} g_{ip}^{(2} \right.$$

$$\left. + \frac{\partial I_5}{\partial x} W_{2ij} + \frac{\partial I_6}{\partial x} W_{3ij} \right) \left. + I_5 \sum_{p=1}^{N} g_{ip}^{(2)} W_{2pj} + I_6 \sum_{p=1}^{N} g \right.$$

$$+ 2V_x^2 \left(\frac{\partial I_3}{\partial x} \sum_{p=1}^{N} g_{ip}^{(1)} W_{0pj} + \frac{\partial I_4}{\partial x} \sum_{p=1}^{N} g_{ip}^{(1)} W_{1pj} \right) + V_x^2 \left(\frac{\partial^2 I_3}{\partial x^2} W_{0ij} + \frac{\partial^2 I_4}{\partial x^2} W_{1ij} \right)$$

$$\left. + \frac{\partial I_5}{\partial x} \sum_{p=1}^{N} g_{ip}^{(1)} W_{2pj} + \frac{\partial I_6}{\partial x} \sum_{p=1}^{N} g_{ip}^{(1)} W_{3pj} \right) \left. + \frac{\partial^2 I_5}{\partial x^2} W_{2ij} + \frac{\partial^2 I_6}{\partial x^2} W_{3ij} \right)$$

(19h)

Where

$$\{A_{ij}, B_{ij}, C_{ij}, D_{ij}, E_{ij}, F_{ij}, G_{ij}\} = \int_0^L \int_{-\frac{h}{2}-c}^{\frac{h}{2}-c} Q_{ij} \{1, z, z^2, z^3, z^4, z^5, z^6\} dz dx \quad i,j = 1,3$$

$$\{A_{ij}, B_{ij}, C_{ij}, D_{ij}, E_{ij}, F_{ij}, G_{ij}\} = \int_0^L \int_{-\frac{h}{2}-c}^{\frac{h}{2}-c} Q_{ij} \{1, z, z^2, z^3, z^4, z^5, z^6\} dz dx \quad i,j = 5$$

(22)

Eqs. (21a-h) in their compact form are as

$$([\mathcal{K}] + i\omega^2[\mathcal{C}] + \omega^2[\mathcal{M}])[U_{0ij} \quad W_{0ij} \quad U_{1ij} \quad W_{1ij} \quad U_{2ij} \quad W_{2ij} \quad U_{3ij} \quad W_{3ij}]^T = 0.$$

(23)

The matrix $\mathcal{K}$, $\mathcal{C}$, and $\mathcal{M}$ in can be written in Appendix section. In addition to, the nontrivial solutions of Eq. (23) are equal to the vibration frequencies of the system. Also, the vibration frequency of the system in dimensionless form can be defined as:

$$\bar{\omega} = \omega L^2 \sqrt{\frac{\rho_c A}{E_c I}},$$

$$\bar{V} = V_x \sqrt{\frac{I}{A}}.$$

(24)

4 NUMERICAL STUDY

4.1. Present Solution Validation

Table 2 to 4 demonstrates the validation of the derived equations in the current study under various boundary conditions.

Table 2 illustrates the natural frequency values based on the parameter nz which represents the degree of gradient in the material function, under clamped-clamped boundary conditions. A comparison is made for clamped-clamped boundary conditions with Ref. [52] (EBBT) and Ref. [52] (TBT) for aspect ratios of 5 and 20. As shown in Table 2, for an aspect ratio of 5, the obtained values closely match those of Ref. [52] (TBT), with a maximum difference occurring at n_z=0, which is less than 4%. However, for L/h=5, the presented model in this study shows significantly larger differences compared to Ref. [52] (EBBT), reaching up to 20% in some cases. On the other hand, for an aspect ratio of 20, the agreement between the results of this study and the reported values in Ref. [52] (EBBT) and Ref. [52] (TBT) is quite satisfactory, with a maximum difference of less than 2%. From this perspective, the present study accurately predicts the natural frequency values for different degrees of material gradient under clamped-clamped boundary conditions.

Table 2

Comparison of the frequency parameters $\left(\bar{\omega} = (\omega L^2/h)\sqrt{(\rho/E)}\right)$ for functionally graded beam with CC edge conditions.

L/h		n_z					
		0	0.2	0.4	0.6	0.8	1
5	Present	5.3675	5.2440	5.2316	5.2110	5.1826	5.1466
	Ref. [52] (EBBT)	6.3291	6.3232	6.3056	6.2763	6.2333	6.1826
	Ref. [52] (TBT)	5.1943	5.1904	5.1806	5.1630	5.1396	5.1083
20	Present	6.3759	6.3544	6.3358	6.3051	6.2627	6.2090
	Ref. [52] (EBBT)	6.4508	6.4434	6.4251	6.3934	6.3494	6.2933
	Ref. [52] (TBT)	6.3486	6.3427	6.3251	6.2939	6.2529	6.2001

Furthermore, according to Table 2, it is evident that the natural frequency of the system increases with an increase in the value of the parameter nz for all cases of L/h. The reason for this increase in natural frequency with an increase in the L/h ratio is that the stiffness matrix of the system improves with this ratio, resulting in a higher natural frequency. Another significant observation inferred from Table 2 is that the natural frequency decreases as the coefficient nz increases in all cases. However, the effect of this parameter on the natural frequency is less pronounced compared to the L/h ratio. The decrease in the natural frequency with an increase in the n_z parameter is attributed to the non-uniform distribution of material properties along different directions of the beam. In the uniform case (n_z=0), the stiffness matrix of the system is more proper compared to the case where the properties vary as a graded function. As the material properties become more non-uniform (higher n_z values), this non-uniformity increases and leads to resistance in the stiffness matrix, ultimately resulting in a decrease in the natural frequency of the system.

On the other hand, Table 3 presents the natural frequency values based on the parameter n_z for clamped-simply boundary conditions, along with Ref. [52] (EBBT) and Ref. [52] (TBT), for aspect ratios of 5 and 20. Similar to the findings from Table 2, it is evident from Table 3 that, for an aspect ratio of 5, the obtained values closely match those of Ref. [52] (TBT), with a maximum difference occurring at n_z=0, which is approximately 2%. However, for an aspect ratio of 5, the presented model in this study shows significantly larger differences compared to Ref. [52] (EBBT), reaching up to 10% in some cases. Conversely, for an aspect ratio of 20, the agreement between the results of this study and the reported values in Ref. [52] (EBBT) and Ref. [52] (TBT) is highly satisfactory, with a maximum difference of less than 1%. From this perspective, the present study predicts the natural frequency values for different degrees of material gradient under clamped-simply boundary conditions with high precision.

Table 3

Comparison of the frequency parameters $\left(\overline{\omega} = (\omega L^2 / h) \sqrt{(\rho/E)} \right)$ for functionally graded beam with CS edge conditions.

L/h		n_z					
		0	0.2	0.4	0.6	0.8	1
5	Present	3.9595	3.9000	3.8920	3.8787	3.8604	3.8372
	Ref. [52] (EBBT)	4.3682	4.3634	4.3511	4.3304	4.3011	4.2657
	Ref. [52] (TBT)	3.8779	3.8759	3.8662	3.8505	3.8310	3.8037
20	Present	4.4169	4.4078	4.3977	4.3810	4.3580	4.3289
	Ref. [52] (EBBT)	4.4451	4.4415	4.4281	4.4061	4.3756	4.3377
	Ref. [52] (TBT)	4.4072	4.4033	4.3896	4.3681	4.3388	4.3017

As previously mentioned in Table 1, by observing Table 3, it can be also stated that, at a specific value of the parameter n_z, the natural frequency of the system exhibits an increasing behavior with an increase in the L/h ratio, and this behavior holds true for all values of n_z. The reason for this increase in natural frequency with an increase in the L/h ratio remains the same, as the stiffness matrix of the system improves with this ratio, leading to higher natural frequencies. Furthermore, from Table 3, it is evident that the natural frequency decreases as the coefficient n_z increases for all cases. However, the effect of this parameter on the natural frequency remains less pronounced compared to the L/h ratio. The underlying reason for this behavior is consistent with what was discussed earlier – in the uniform case (n_z=0), the stiffness matrix of the system is more favorable compared to the case where the properties vary as a graded function. As the material properties become more non-uniform (higher n_z values), this non-uniformity increases and results in resistance in the stiffness matrix, ultimately leading to a decrease in the natural frequency of the system.

Finally, Table 4 presents the natural frequency values based on the parameter nz for clamped-free boundary conditions, along with Ref. [52] (EBBT) and Ref. [52] (TBT), for aspect ratios of 5 and 20. According to Table 4, it is evident that, for an aspect ratio of 5, the obtained values closely match those of both Ref. [52] (EBBT) and Ref. [52] (TBT), with a maximum difference occurring at $n_z=0$, which is approximately 1%. In this case, as the value of nz increases from smaller to larger values, the difference between the results decreases. Moreover, for an aspect ratio of 20, there is excellent agreement between the results of this study and the reported values in Ref. [52] (EBBT) and Ref. [52] (TBT), with a maximum difference of less than 1%. From this point of view, the present study predicts the natural frequency values for different degrees of material gradient under clamped-free boundary conditions with high precision.

As indicated in Table 4, at a specific value of the parameter n_z, the natural frequency of the system exhibits an increasing behavior with an increase in the L/h ratio, and this behavior holds true for all values of n_z. The reason for this increase in natural frequency with an increase in the L/h ratio remains the same: the stiffness matrix of the system improves with this ratio, resulting in higher natural frequencies. Furthermore, from Table 3, it is evident that the natural frequency decreases as the coefficient n_z increases for all cases. The reason for this behavior is consistent with what was discussed earlier – in the uniform case ($n_z=0$), the stiffness matrix of the system is higher compared to the case where the properties vary as a graded function. As the material properties become more non-uniform (higher n_z values), this non-uniformity increases and leads to resistance in the stiffness matrix, ultimately resulting in a decrease in the natural frequency of the system. It is worth noting that the influence of n_z on the natural frequency is less pronounced compared to the effect of the L/h ratio.

Table 4

Comparison of the frequency parameters $\left(\bar{\omega} = (\omega L^2 / h) \sqrt{(\rho/E)} \right)$ for functionally graded beam with CF edge conditions.

L/h		n_z					
		0	0.2	0.4	0.6	0.8	1
	Present	0.9910	0.9865	0.9836	0.9790	0.9725	0.9644
5	Ref. [52] (EBBT)	1.0068	1.0068	1.0029	0.9990	0.9912	0.9833
	Ref. [52] (TBT)	0.9844	0.9832	0.9796	0.9735	0.9661	0.9576
	Present	1.0162	1.0111	1.0081	1.0031	0.9963	0.9877
20	Ref. [52] (EBBT)	1.0146	1.0126	1.0107	1.0048	0.9990	0.9892
	Ref. [52] (TBT)	1.0126	0.0126	1.0087	1.0029	0.9970	0.9873

4.2. Convergence study

As previously mentioned, DQM was used to solve the equations of the presented analysis model. Table 5 demonstrates the convergence behavior for the number of points in the DQM for each of the boundary conditions: clamped-clamped, clamped-simply, and clamped-free.

Table 5

Convergence of fundamental frequency of the bi-directionally graded moving beams.

	N_x							
	6	8	10	12	14	16	18	20
CC	13.23	12.64	12.62	12.60	12.59	12.59	12.59	12.59
CS	8.67	8.68	8.67	8.67	8.67	8.67	8.68	8.68
SS	5.48	5.57	5.57	5.57	5.57	5.57	5.57	5.57

Table 6

The impacts of mode number on the dimensionless frequency of various supported bi-directionally graded moving beams.

	Mode 1	Mode 2	Mode 3	Mode 4	Mode 5	Mode 6
CC	10.2991	26.4489	47.9106	53.5095	72.9153	100.2954
CS	7.2740	22.2394	43.1435	51.5774	68.1822	95.8456
SS	4.7622	18.1622	38.3534	49.7363	63.3180	91.2094
CF	1.7107	10.2418	26.6536	27.0904	49.0603	74.7426

According to Table 5, it is evident that, for a specific number of points, as we move from the simply-simply boundary condition towards the clamped-clamped condition, the convergence value increases. This implies that, in general, fewer points are required to achieve convergence when the boundary conditions have more constraints and fewer degrees of freedom. In other words, for the simply-simply boundary condition, which has more degrees of freedom and fewer constraints compared to the clamped-clamped condition, a higher number of points is required to achieve the desired convergence. To show the effect of mode number, and boundary conditions on the dimensionless frequency of the bi-directionally graded moving beam, Table 6 is presented. As is observed in this table, by increasing the mode number, the dimensionless frequency increases. Also, clamped-clamped (CC) boundary conditions due to high rigidity in boundary edges has higher dimensionless frequency than other types of boundary conditions.

4.3. Parametric study

The behavior of the dimensionless natural frequency ($\bar{\omega} = \omega L^2 \sqrt{\frac{\rho_c A}{E_c I}}$) as a function of different L/h ratios is

shown in Figure 2 for various moving velocities and under clamped-clamped boundary conditions. According to Figure 2, both parameters, L/h, and the average velocity, significantly influence the natural frequency of the material. For velocities of 0 and 1, after an initial increase (from L/h=10 to 20), the natural frequency remains relatively constant at approximately 12 to 12.5 for other L/h values. In other words, when the velocity is either 0 or

1, the natural frequency becomes independent of L/h values greater than 20. On the other hand, for velocities of 2 and 3, the natural frequency first increases and then exhibits a decreasing behavior. The maximum reported natural frequency is consistently associated with lower velocities, such that at any chosen L/h ratio, the natural frequency decreases with an increase in velocity. According to Figure 2, it is evident that, in general, for a specific L/h ratio, the natural frequency experiences a decrease, and system instability increases with an increase in axial velocity. Although the behaviors vary at different velocities, the overall trend shows a consistent reduction in the natural frequency with increasing axial velocity.

Figure 3 illustrates the behavior of the dimensionless natural frequency ($\overline{\omega} = \omega L^2 \sqrt{\frac{\rho_c A}{E_c I}}$) as a function of various L/h ratios for different moving velocities under clamped-simply boundary conditions. Similar to the observations in Figure 2, both parameters, L/h and the average velocity, significantly influence the natural frequency of the material.

For velocities of 0 and 1, after an initial increase (from L/h=10 to 30), the natural frequency remains nearly constant at approximately 8.4 to 8.6 for other L/h values. On the other hand, for velocities of 2 and 3, the natural frequency first increases and then exhibits a decreasing trend. This decreasing behavior is particularly pronounced for the velocity of 3. Additionally, it is evident that the reported maximum natural frequency consistently corresponds to lower velocities. Specifically, for any chosen L/h ratio, an increase in velocity leads to a reduction in the natural frequency. As stated earlier, similar to the observations in Figure 2, Figure 3 also indicates that, in general, for a specific L/h ratio, the natural frequency experiences a decrease, and system instability increases with an increase in axial velocity. Although the behaviors vary at different velocities, the overall trend consistently shows a reduction in the natural frequency with increasing axial velocity.

Figure 4 depicts the behavior of the dimensionless natural frequency as a function of various L/h ratios for different moving velocities under simply-simply boundary conditions. Similar to the observations in Figure 3, it can be deduced from Figure 4 that both parameters, L/h, and the average velocity, significantly influence the natural frequency of the system. For velocities of 0 and 1, the natural frequency remains nearly constant across all L/h values. In other words, when the velocity is either 0 or 1, the natural frequency remains unaffected by changes in L/h. On the other hand, for velocities of 2 and 3, the natural frequency exhibits a decreasing trend without displaying a clear extremum. This decreasing behavior is particularly pronounced for the velocity of 3. Consistent with previous observations, Figure 4 also demonstrates that the reported maximum natural frequency corresponds to lower velocities. Specifically, for any chosen L/h ratio, an increase in velocity leads to a reduction in the natural frequency.

Figure 5 illustrates the behavior of the dimensionless natural frequency as a function of various L/h ratios for different moving velocities under clamped-free boundary conditions. In contrast to the observations in Figure 4, at the velocity of 0, the natural frequency is not constant across all L/h values. Instead, it exhibits an increasing trend in almost all L/h ratios, except for large L/h values. Similarly, for the velocity of 1, the natural frequency shows a gently increasing trend and reaches its maximum around L/h approximately equal to 35, after which it displays a decreasing behavior. Consistent with previous findings, velocities 2 and 3 show decreasing trends in the natural frequency without displaying a clear extremum. This decreasing behavior is particularly significant for the velocity of 3. Also, Figure 5 highlights that the reported maximum natural frequency corresponds to lower velocities. Regardless of the chosen L/h ratio, an increase in velocity leads to a reduction in the natural frequency.
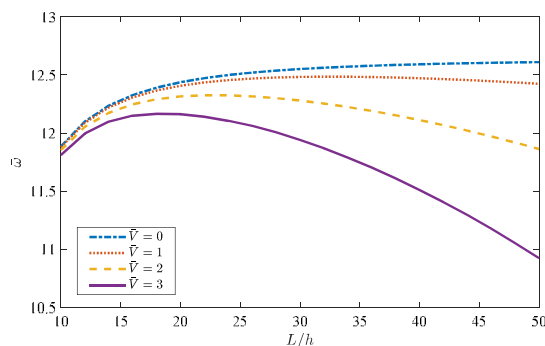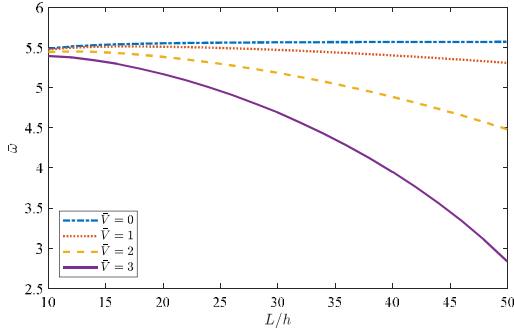

Fig. 2
The impacts of L/h, and $\overline{V}$ on the dimensionless frequency of CC-supported bi-directionally graded moving beams.
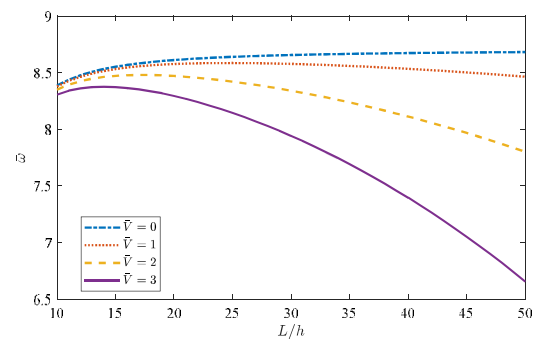
Fig. 3
The impacts of L/h, and $\overline{V}$ on the dimensionless frequency of CS-supported bi-directionally graded moving beams.

Fig. 4

The impacts of L/h, and $\bar{V}$ on the dimensionless frequency of SS-supported bi-directionally graded moving beams.
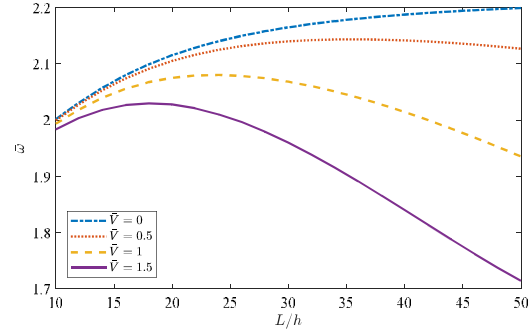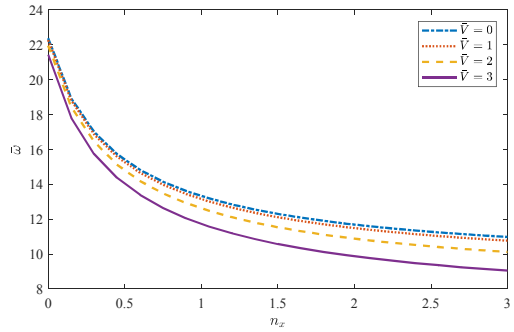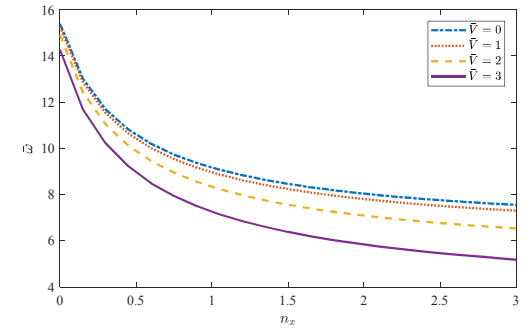

Fig. 5

The impacts of L/h, and $\bar{V}$ on the dimensionless frequency of CF-supported bi-directionally graded moving beams.

Fig. 6

The impacts of n_x, and $\bar{V}$ on the dimensionless frequency of CC-supported bi-directionally graded moving beams.

Fig. 7

The impacts of n_x, and $\bar{V}$ on the dimensionless frequency of CS-supported bi-directionally graded moving beams.

The comparison of Figures 2 to 5 also reveals that despite similar trends in different moving velocities across all boundary conditions, the type of boundary condition significantly affects the magnitude of the natural frequency. Specifically, the highest natural frequencies occur under clamped-clamped boundary conditions, while the lowest frequencies are observed under clamped-free boundary conditions. The intermediate values are observed for clamped-simply and simply-simply boundary conditions. Another crucial point to note in comparing Figures 2 to 5 is that changing the boundary conditions from simply-simply to clamped-clamped drives the maximum natural frequency at the velocity of 3 towards smaller values of L/h. Additionally, transitioning from simply-simply to clamped-clamped boundary conditions consistently results in increasing natural frequency values. For instance, at L/h = 10, the natural frequency value for clamped-free boundary condition is approximately 2.5, for simply-simply it is around 5.5 at all velocities, for clamped-simply it is 8.5, and for clamped-clamped it is 12.5. Furthermore, a general observation from Figures 2 to 5 is that the influence of the axial velocity on the natural frequency is dependent on the parameter L/h. For lower values of L/h (between 10 to 20), an increase in axial velocity has a minimal impact on the variation of natural frequency. However, for higher values of L/h, the natural frequency undergoes significant changes with variations in axial velocity.

Figure 6 illustrates the behavior of dimensionless natural frequency concerning the parameter of the graded function, n_x, for various axial velocities when the boundary conditions are clamped-clamped. According to the depicted diagram, as the parameter n_x increases, the natural frequency decreases for all velocities. This decrease initially occurs at a steep rate and then gradually decreases in intensity with further increments of n_x. On the other hand, as shown in Figure 6, with an increase in axial velocity, the natural frequency values decrease. However, the effect of axial velocity on the reduction of the natural frequency is significantly lower compared to the impact of the n_x parameter.

Figure 7 depicts the behavior of dimensionless natural frequency concerning the parameter of the graded function, n_x, for various axial velocities under clamped-simply boundary conditions. Similar to the observations made earlier for Figure 6, it is evident from Figure 7 that an increase in the n_x parameter leads to a reduction in the natural frequency for all velocities. This decrease initially occurs at a steep rate and then gradually decreases in intensity with further increments of n_x. Moreover, in accordance with Figure 7, an increase in axial velocity results

in a decrease in the natural frequency values. However, the effect of axial velocity on the reduction of the natural frequency is significantly lower compared to the impact of the n_x parameter.

Figure 8 also illustrates the behavior of dimensionless natural frequency concerning the parameter of the graded function, n_x, for various axial velocities, this time under simply-simply boundary conditions. Similar to the previous figures (6 and 7), Figure 8 shows that an increase in the n_x parameter leads to a reduction in the natural frequency for all velocities. This decrease initially occurs at a steep rate and then gradually decreases in intensity with further increments of n_x. However, a notable distinction in this figure compared to Figures 6 and 7 is that the effect of increasing axial velocity on the behavior of the natural frequency is more pronounced. In other words, for a specific value of n_x, the difference in natural frequency between different axial velocities is greater in this simply-simply boundary condition than in the previous two cases.

Figure 9 presents the behavior of dimensionless natural frequency concerning the parameter of the graded function, n_x, for various axial velocities, this time under clamped-free boundary conditions. Similar to the previous figures (6, 7, and 8), Figure 9 shows that an increase in the n_x parameter results in a reduction in the natural frequency for all velocities. This decrease occurs initially at a steep rate and intensifies further with greater increments of n_x. Furthermore, as depicted in Figure 9, with an increase in axial velocity, the values of the natural frequency decrease. However, the effect of axial velocity on the reduction of natural frequency is relatively smaller compared to the impact of the n_x parameter. In addition, a consistent observation similar to Figures 6-8 is that with increasing velocity at any specific value of n_x, the natural frequency decreases.
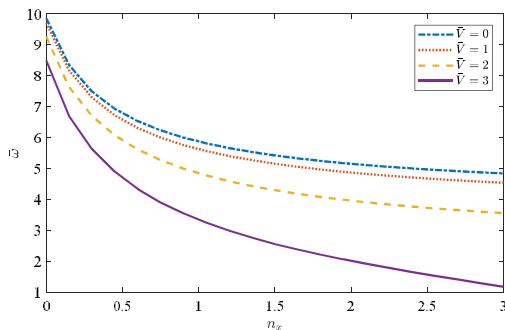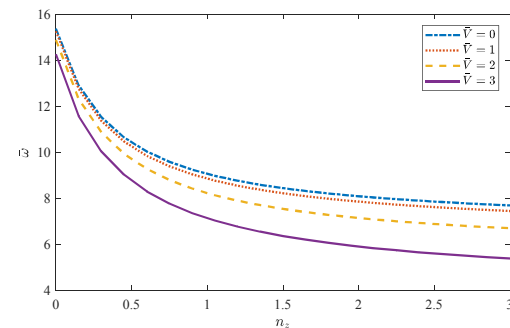

Fig. 8

The impacts of n_x, and $\overline{V}$ on the dimensionless frequency of SS-supported bi-directionally graded moving beams.
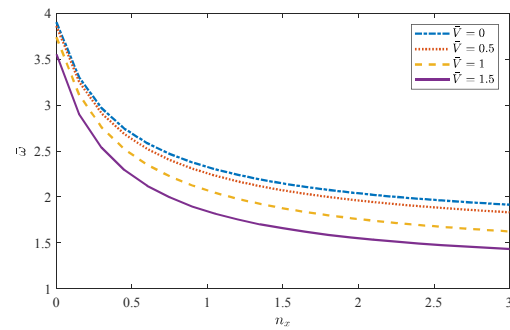
Fig. 9

The impacts of n_x, and $\overline{V}$ on the dimensionless frequency of CF-supported bi-directionally graded moving beams.
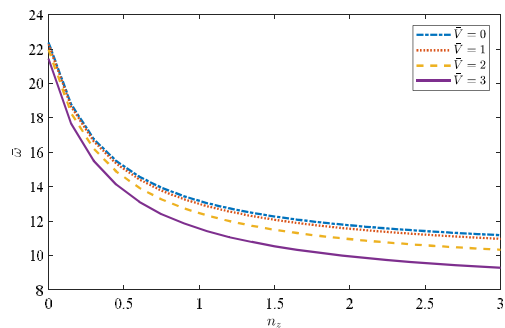
Fig. 10

The impacts of n_z, and $\overline{V}$ on the dimensionless frequency of CC-supported bi-directionally graded moving beams.

Fig. 11

The impacts of n_z, and $\overline{V}$ on the dimensionless frequency of CS-supported bi-directionally graded moving beams.

By comparing Figures 6 to 9, it is evident that the effect of the axial velocity parameter is also dependent on the type of boundary condition. Specifically, in the clamped-clamped boundary condition, the influence of changes in axial velocity on the natural frequency is less pronounced compared to the simply-simply boundary condition. This behavior can be attributed to the fact that, as depicted in the figures, the diagrams for the clamped-clamped boundary condition are much closer to each other, while in the simply-simply condition, they show greater separation. Additionally, it is evident that in all boundary conditions, the effect of n_x and n_z parameters is much more significant at the beginning of the range of variation than in the later part of the range. This indicates that the impact

of these parameters is more pronounced in the initial stages of their variations. Indeed, variations in these coefficients within the range from 0 to 0.5 can lead to changes in natural frequencies of up to approximately 100%. Notably, changes in the n_x parameter from 0.5 to 3 can only cause variations of around 30% in natural frequencies. This behavior intensifies with increasing axial velocity. For example, in the case of a beam with simply-simply boundary conditions and an axial velocity of 3, increasing the n_x coefficient from 0 to 0.5 results in a decrease in natural frequency from 8.5 to 4.5 (approximately 100% change). However, for an axial velocity of 1, the same change in n_x leads to a decrease in natural frequency from 10 to 7 (approximately 35% change). Therefore, the effectiveness of the n_x parameter, especially in smaller ranges of axial velocity, is dependent on the value of the axial velocity itself. The higher the axial velocity, the more significant the impact of changes in n_x on the natural frequencies.

Figure 10 illustrates the behavior of the dimensionless natural frequency with respect to the varying parameter of the gradation function, n_z, for different axial velocities under the boundary conditions of simply-supported beams. Similar to Figures 9 and 8, it is evident that as the n_z parameter increases, the natural frequency decreases for all velocities. This decrease occurs rapidly initially, and its intensity diminishes with further increments of n_z. Additionally, increasing the axial velocity leads to a reduction in the natural frequency values, although the influence of velocity is significantly less pronounced compared to the effect of the n_z parameter.

Figure 11 presents the behavior of the dimensionless natural frequency concerning the parameter of the gradation function, n_z, for various axial velocities under the boundary conditions of clamped-free beams. As depicted in Figure 11, it can be deduced that the natural frequency decreases with an increase in the nz parameter for all velocities. This decrease exhibits a steep initial decline, and its intensity further diminishes with higher values of n_z. Moreover, in accordance with Figure 11, the natural frequency values decrease with increasing axial velocity, although the influence of velocity on the reduction of the natural frequency is notably less significant compared to the effect of the n_z parameter. Additionally, with an increase in the axial velocity for any given value of n_z, the magnitude of the natural frequency also decreases.

Figure 12 illustrates the behavior of the dimensionless natural frequency with respect to the parameter of the gradation function, n_z, for various axial velocities under the boundary conditions of simply-supported beams. As observed in Figure 12, it is evident that the natural frequency decreases as the n_z parameter increases for all velocities. This decrease exhibits a steep initial decline, and its intensity further diminishes with higher values of n_z. A distinct feature of this figure, as compared to Figures 10 and 11, is the heightened impact of increasing axial velocity on the behavior of the natural frequency. In other words, for a specific value of n_z, the discrepancy in natural frequency among different velocities is greater in these simply-supported boundary conditions than in the previous cases.

To show the dimensionless frequency response of the SS-supported bi-directionally graded moving beam for different n_z, n_x, and boundary conditions Figs. 13-16 are appeared. As can be seen in Figs. 13-16, by increasing the FG power index in each direction, the dimensionless frequency decreases. In n_z equal to 0, decreasing the dimensionless frequency due to increasing n_x parameter is more obvious than other values of n_z parameter. By comparing the results of Figs. 13-16 can be concluded that by changing the boundary conditions of the presented composite structure from CC to CF, the stability and finally the dimensionless frequency decreases. This is because, by changing the boundary conditions from clamped to simply or free, the rigidity of the boundary conditions decreases and finally, the dimensionless frequency of the system decreases.
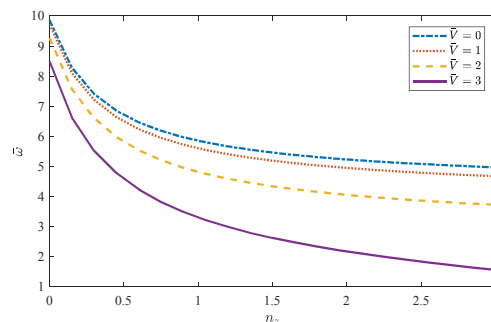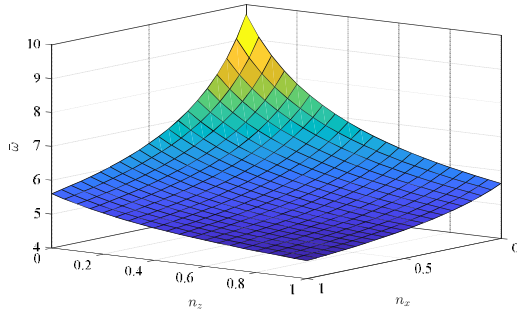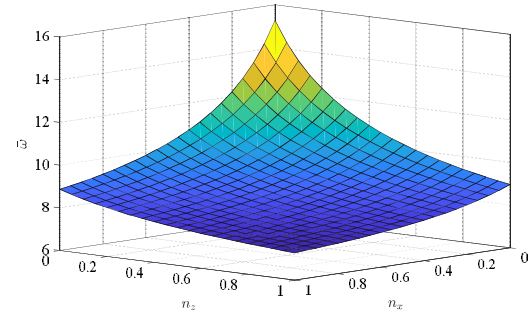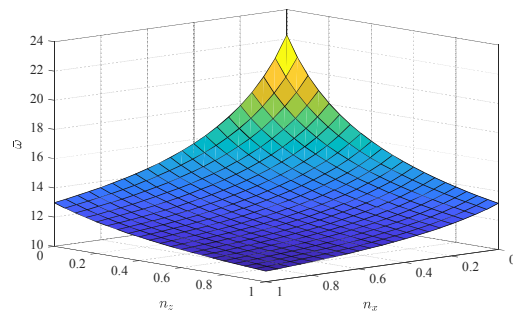

Fig. 12

The impacts of n_z, and $\bar{V}$ on the dimensionless frequency of SS-supported bi-directionally graded moving beams.

Fig. 13

The impacts of n_z, and n_x on the dimensionless frequency of SS-supported bi-directionally graded moving beams.

Fig. 14

The impacts of n_z, and n_x on the dimensionless frequency of CS-supported bi-directionally graded moving beams.
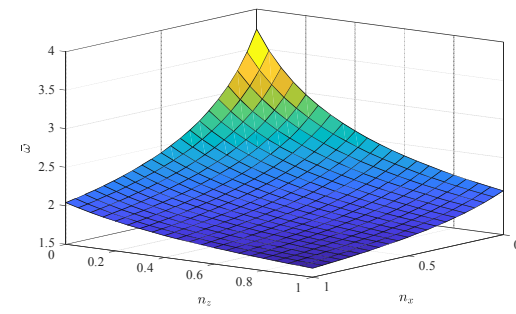

Fig. 15

The impacts of n_z, and n_x on the dimensionless frequency of CC-supported bi-directionally graded moving beams.

Fig. 16

The impacts of n_z, and n_x on the dimensionless frequency of CF-supported bi-directionally graded moving beams.

5   CONCLUSIONS

This article gravitates toward analyzing the vibration response of a moving beam functionally graded in two orthogonal directions. In order to gain a high level of accuracy, higher-order shear deformation theory for beam structures is employed to define the displacement field and determine the system's governing differential equations. Also, this study considers the effect of different sets of boundary conditions to find the oscillatory response of the system in a more comprehensive way. This matter leads the authors to utilize DQM as a numerical solution to solve the governing differential equations. The most significant scientific results of this study are briefly listed as follows:

- In this study, the natural frequency of a moving beam with varying properties along both the axial and transverse directions was investigated. The study examined the influence of boundary conditions, gradational properties, axial velocity, and the parameter L/h on the natural frequency.
- With an increase in the gradational property parameter (nx/nz), the average elastic coefficient of the system decreases. In other words, the highest elastic coefficient is obtained in the case of uniform properties, while the presence of gradational variations in both directions leads to the lowest elastic coefficient.
- With an increase in the gradational property parameter (nx/nz), the average density of the system increases. In other words, the lowest density is present in the case of uniform properties, whereas the highest density is observed when gradational variations exist in both directions. This phenomenon can be attributed to the fact that the density of the gradational factor is higher than that of the base material.
- With an increase in the gradational property parameter (nx/nz), the average Poisson's ratio of the system increases. In other words, the lowest Poisson's ratio is present in the case of uniform properties, whereas the highest Poisson's ratio is observed when gradational variations exist in both directions. This phenomenon can be attributed to the fact that the gradational factor has a higher density compared to the base material.

- In general, for a specific aspect ratio (L/h), an increase in axial velocity results in a decrease in the natural frequency and an increase in system instability. Although behaviors vary at different velocities, the natural frequency consistently decreases with increasing axial velocity. This phenomenon can be attributed to the similarity between the increase in velocity in moving axial beams and the increase in pressure in columns, leading to an escalation in system instability with higher velocities.

- The effect of the aspect ratio (L/h) on the natural frequency is somewhat complex and is dependent on the axial velocity. Within the studied range and at lower velocities, the natural frequency increases with an increase in the l/h ratio. This increase is more pronounced at smaller l/h values and gradually diminishes, leading to a nearly constant natural frequency. On the other hand, at higher velocities, the natural frequency initially increases with an increase in l/h, but then decreases, resulting in a graph with an extremum point.

- The decreasing behavior of the natural frequency in comparison to the increasing behavior exhibits a higher magnitude. As the L/h ratio changes, a significant reduction in the natural frequency occurs, showcasing a more pronounced effect on the system's behavior.
  The effect of boundary conditions on the natural frequency is clearly evident. Generally, with a change in the boundary conditions towards clamped-clamped, the natural frequency values consistently increase. The lowest natural frequency occurs for the clamped-free boundary conditions. The next in line is the simply-simply boundary conditions, followed by the clamped-simply conditions. Lastly, the highest natural frequency corresponds to the clamped-clamped boundary conditions.
  In general, the introduction of gradient (n_x/n_z) properties results in a reduction of the natural frequency of the system, leading to increased system instability. Additionally, the results indicate that in all boundary conditions, the effect of nx and nz is much more significant at the beginning of the range of change compared to the rest of the range. Specifically, changes in nx from 0.5 to 3 can only induce approximately 30% variation in the natural frequency. However, this behavior intensifies with increasing axial velocity. For instance, in the case of a beam with simple-simple boundary conditions and an axial velocity of 3, increasing the nx coefficient from 0 to 0.5 causes the natural frequency to decrease from 8.5 to 4.5 (approximately 100% change). On the other hand, for an axial velocity of 1, the natural frequency decreases from 10 to 7 (approximately 35%) with the same change in the nx coefficient. Thus, the influence of nx, particularly in lower ranges, is strongly dependent on the axial velocity.

- The effect of velocity on the real and imaginary parts of the natural frequencies is as follows: When the beam's velocity is zero, the natural frequencies of the system are entirely real. As the velocity increases, the real part of the natural frequencies gradually decreases while their imaginary part remains zero. At the critical velocity, the real part of the fundamental natural frequency becomes zero, indicating the loss of stability in the system. The induced instability, similar to buckling in classic compressed columns, is due to divergence in axially moving systems, where the increase in axial velocity is analogous to the interpretation of compressive force in columns. As expected, in columns, increasing the axial force and reaching a critical force leads to buckling. Similarly, in this scenario, with increasing axial velocity and reaching the critical velocity, the real part of the natural frequencies is diminished, leading to increased instability. With a further increase in velocity, the fundamental natural frequency becomes completely imaginary, while the third natural frequency decreases uniformly. In this case, due to gyroscopic effects, the system regains its stability. It can be stated that the initiation and termination points of the first mode divergence instability are associated with the disappearance of the real and imaginary parts of the fundamental natural frequency, respectively.

6 APPENDIX

The matrix $\mathcal{K}$, $\mathcal{C}$, and $\mathcal{M}$ in Eq. (23) can be written as follows:

$$\mathcal{K} = \lfloor \mathcal{K}_{ij} \rfloor, \quad \mathcal{C} = \lfloor \mathcal{C}_{ij} \rfloor, \quad \mathcal{M} = \lfloor \mathcal{M}_{ij} \rfloor, \quad i,j = 1,\dots,8.$$

$$\mathcal{K}_{11} = A_{11} \sum_{\wp=1}^{N} g_{i\wp}^{(2)} U_{0\wp j} + A_{11}^{(1)} \sum_{\wp=1}^{N} g_{i\wp}^{(1)} U_{0\wp j} + V_x^2 I_0 \sum_{\wp=1}^{N} g_{i\wp}^{(2)} U_{0\wp j}$$

$$+2V_x^2 \frac{\partial I_0}{\partial x} \sum_{p=1}^{N} g_{ip}^{(1)} U_{0pj} + V_x^2 \frac{\partial^2 I_0}{\partial x^2} U_{0ij},$$

$$\mathcal{K}_{12} = 0,$$

$$\mathcal{K}_{13} = B_{11} \sum_{p=1}^{N} g_{ip}^{(2)} U_{1pj} + B_{11}^{(1)} \sum_{p=1}^{N} g_{ip}^{(1)} U_{1pj} + V_x^2 I_1 \sum_{p=1}^{N} g_{ip}^{(2)} U_{1pj}$$

$$+2V_x^2 \frac{\partial I_1}{\partial x} \sum_{p=1}^{N} g_{ip}^{(1)} U_{1pj} + V_x^2 \frac{\partial^2 I_1}{\partial x^2} U_{1ij},$$

$$\mathcal{K}_{14} = A_{13} \sum_{p=1}^{N} g_{ip}^{(1)} W_{1pj} + A_{13}^{(1)} \sum_{p=1}^{N} I_{ip} W_{1pj},$$

$$\mathcal{K}_{15} = C_{11} \sum_{p=1}^{N} g_{ip}^{(2)} U_{2pj} + C_{11}^{(1)} \sum_{p=1}^{N} g_{ip}^{(1)} U_{2pj} + V_x^2 I_2 \sum_{p=1}^{N} g_{ip}^{(2)} U_{2pj}$$

$$+2V_x^2 \frac{\partial I_2}{\partial x} \sum_{p=1}^{N} g_{ip}^{(1)} U_{2pj} + V_x^2 \frac{\partial^2 I_2}{\partial x^2} U_{2ij},$$

$$\mathcal{K}_{16} = 2B_{13} \sum_{p=1}^{N} g_{ip}^{(1)} W_{2pj} + 2B_{13}^{(1)} \sum_{p=1}^{N} I_{ip} W_{2pj},$$

$$\mathcal{K}_{17} = D_{11} \sum_{p=1}^{N} g_{ip}^{(2)} U_{3pj} + D_{11}^{(1)} \sum_{p=1}^{N} g_{ip}^{(1)} U_{3pj} + V_x^2 I_3 \sum_{p=1}^{N} g_{ip}^{(2)} U_{3pj}$$

$$+2V_x^2 \frac{\partial I_3}{\partial x} \sum_{p=1}^{N} g_{ip}^{(1)} U_{3pj} + V_x^2 \frac{\partial^2 I_3}{\partial x^2} U_{3ij},$$

$$\mathcal{K}_{18} = 3C_{13} \sum_{p=1}^{N} g_{ip}^{(1)} W_{3pj} + 3C_{13}^{(1)} \sum_{p=1}^{N} I_{ip} W_{3pj},$$

$$\mathcal{K}_{21} = 0,$$

$$\mathcal{K}_{22} = A_{55} \sum_{p=1}^{N} g_{ip}^{(2)} W_{0pj} + A_{55}^{(1)} \sum_{p=1}^{N} g_{ip}^{(1)} W_{0pj} + V_x^2 I_0 \sum_{p=1}^{N} g_{ip}^{(2)} W_{0pj}$$

$$+2V_x^2 \frac{\partial I_0}{\partial x} \sum_{p=1}^{N} g_{ip}^{(1)} W_{0pj} + V_x^2 \frac{\partial^2 I_0}{\partial x^2} W_{0ij},$$

$$\mathcal{K}_{23} = A_{55} \sum_{p=1}^{N} g_{ip}^{(1)} U_{1pj} + A_{55}^{(1)} \sum_{p=1}^{N} I_{ip} U_{1pj},$$

$$\mathcal{K}_{24} = C_{55} \sum_{p=1}^{N} g_{ip}^{(2)} W_{2pj} + B_{55}^{(1)} \sum_{p=1}^{N} g_{ip}^{(1)} W_{1pj} + V_x^2 I_1 \sum_{p=1}^{N} g_{ip}^{(2)} W_{1pj}$$

$$+2V_x^2 \frac{\partial I_1}{\partial x} \sum_{p=1}^{N} g_{ip}^{(1)} W_{1pj} + V_x^2 \frac{\partial^2 I_1}{\partial x^2} W_{1ij},$$

$$\mathcal{K}_{25} = 2B_{55} \sum_{p=1}^{N} g_{ip}^{(1)} U_{2pj} + 2B_{55}^{(1)} \sum_{p=1}^{N} I_{ip} U_{2pj},$$

$$\mathcal{K}_{26} = C_{55} \sum_{p=1}^{N} g_{ip}^{(2)} W_{2pj} + C_{55}^{(1)} \sum_{p=1}^{N} g_{ip}^{(1)} W_{2pj} + V_x^2 I_2 \sum_{p=1}^{N} g_{ip}^{(2)} W_{2pj}$$

$$+2V_x^2 \frac{\partial I_2}{\partial x} \sum_{p=1}^{N} g_{ip}^{(1)} W_{2pj} + V_x^2 \frac{\partial^2 I_2}{\partial x^2} W_{2ij},$$

$$\mathcal{K}_{27} = 3C_{55} \sum_{p=1}^{N} g_{ip}^{(1)} U_{3pj} + 3C_{55}^{(1)} \sum_{p=1}^{N} I_{ip} U_{3pj},$$

$$\mathcal{K}_{28} = D_{55} \sum_{p=1}^{N} g_{ip}^{(2)} W_{3pj} + D_{55}^{(1)} \sum_{p=1}^{N} g_{ip}^{(1)} W_{3pj} + V_x^2 I_3 \sum_{p=1}^{N} g_{ip}^{(2)} W_{3pj}$$

$$+ 2V_x^2 \frac{\partial I_3}{\partial x} \sum_{p=1}^{N} g_{ip}^{(1)} W_{3pj} + V_x^2 \frac{\partial^2 I_3}{\partial x^2} W_{3ij},$$

$$\mathcal{K}_{31} = B_{11} \sum_{p=1}^{N} g_{ip}^{(2)} U_{0pj} + B_{11}^{(1)} \sum_{p=1}^{N} g_{ip}^{(1)} U_{0pj} + V_x^2 I_1 \sum_{p=1}^{N} g_{ip}^{(2)} U_{0pj}$$

$$+ 2V_x^2 \frac{\partial I_1}{\partial x} \sum_{p=1}^{N} g_{ip}^{(1)} U_{0pj} + V_x^2 \frac{\partial^2 I_1}{\partial x^2} U_{0ij}$$

$$\mathcal{K}_{32} = -A_{55} \sum_{p=1}^{N} g_{ip}^{(1)} W_{0pj}$$

$$\mathcal{K}_{33} = C_{11} \sum_{p=1}^{N} g_{ip}^{(2)} U_{1pj} + C_{11}^{(1)} \sum_{p=1}^{N} g_{ip}^{(1)} U_{1pj} - A_{55} U_{1ij} + V_x^2 I_2 \sum_{p=1}^{N} g_{ip}^{(2)} U_{1pj}$$

$$+ 2V_x^2 \frac{\partial I_2}{\partial x} \sum_{p=1}^{N} g_{ip}^{(1)} U_{1pj} + V_x^2 \frac{\partial^2 I_2}{\partial x^2} U_{1ij}$$

$$\mathcal{K}_{34} = B_{13} \sum_{p=1}^{N} g_{ip}^{(1)} W_{1pj} + B_{13}^{(1)} \sum_{p=1}^{N} I_{ip} W_{1pj} - B_{55} \sum_{p=1}^{N} g_{ip}^{(1)} W_{1pj}$$

$$\mathcal{K}_{35} = D_{11} \sum_{p=1}^{N} g_{ip}^{(2)} U_{2pj} + D_{11}^{(1)} \sum_{p=1}^{N} g_{ip}^{(1)} U_{2pj} - 2B_{55} U_{2ij} + V_x^2 I_3 \sum_{p=1}^{N} g_{ip}^{(2)} U_{2pj}$$

$$+ 2V_x^2 \frac{\partial I_3}{\partial x} \sum_{p=1}^{N} g_{ip}^{(1)} U_{2pj} + V_x^2 \frac{\partial^2 I_3}{\partial x^2} U_{2ij}$$

$$\mathcal{K}_{36} = 2C_{13} \sum_{p=1}^{N} g_{ip}^{(1)} W_{2pj} + 2C_{13}^{(1)} \sum_{p=1}^{N} I_{ip} W_{2pj} - C_{55} \sum_{p=1}^{N} g_{ip}^{(1)} W_{2pj}$$

$$\mathcal{K}_{37} = E_{11} \sum_{p=1}^{N} g_{ip}^{(2)} U_{3pj} + E_{11}^{(1)} \sum_{p=1}^{N} g_{ip}^{(1)} U_{3pj} - 3C_{55} U_{3ij} + V_x^2 I_4 \sum_{p=1}^{N} g_{ip}^{(2)} U_{3pj}$$

$$+ 2V_x^2 \frac{\partial I_4}{\partial x} \sum_{p=1}^{N} g_{ip}^{(1)} U_{3pj} + V_x^2 \frac{\partial^2 I_4}{\partial x^2} U_{3ij}$$

$$\mathcal{K}_{38} = 3D_{13} \sum_{p=1}^{N} g_{ip}^{(1)} W_{3pj} + 3D_{13}^{(1)} \sum_{p=1}^{N} I_{ip} W_{3pj} - D_{55} \sum_{p=1}^{N} g_{ip}^{(1)} W_{3pj}$$

$$\mathcal{K}_{41} = -A_{13} \sum_{p=1}^{N} g_{ip}^{(1)} U_{0pj},$$

$$\mathcal{K}_{42} = B_{55} \sum_{p=1}^{N} g_{ip}^{(2)} W_{0pj} + B_{55}^{(1)} \sum_{p=1}^{N} g_{ip}^{(1)} W_{0pj} - V_x^2 I_1 \sum_{p=1}^{N} g_{ip}^{(2)} W_{0pj} - 2V_x^2 \frac{\partial I_1}{\partial x} \sum_{p=1}^{N} g_{ip}^{(1)} W_{0pj} - V_x^2 \frac{\partial^2 I_1}{\partial x^2} W_{0ij}$$

,

$$\mathcal{K}_{43} = B_{55} \sum_{p=1}^{N} g_{ip}^{(1)} U_{1pj} + B_{55}^{(1)} \sum_{p=1}^{N} I_{ip} U_{1pj} - B_{13} \sum_{p=1}^{N} g_{ip}^{(1)} U_{1pj},$$

$$\mathcal{K}_{44} =$$
$$C_{55} \sum_{p=1}^{N} g_{ip}^{(2)} W_{1pj} + C_{55}^{(1)} \sum_{p=1}^{N} g_{ip}^{(1)} W_{1pj} - A_{33} W_{1ij} - V_x^2 I_2 \sum_{p=1}^{N} g_{ip}^{(2)} W_{1pj} - 2V_x^2 \frac{\partial I_2}{\partial x} \sum_{p=1}^{N} g_{ip}^{(1)} W_{1pj} - V_x^2 \frac{\partial^2 I_2}{\partial x^2} W_{1ij}$$

,

$$\mathcal{K}_{45} = 2C_{55} \sum_{p=1}^{N} g_{ip}^{(1)} U_{2pj} + 2C_{55}^{(1)} \sum_{p=1}^{N} I_{ip} U_{2pj} - C_{13} \sum_{p=1}^{N} g_{ip}^{(1)} U_{2pj},$$

$$\mathcal{K}_{46} =$$
$$D_{55} \sum_{p=1}^{N} g_{ip}^{(2)} W_{2pj} + D_{55}^{(1)} \sum_{p=1}^{N} g_{ip}^{(1)} W_{2pj} - 2B_{33} W_{2ij} - V_x^2 I_3 \sum_{p=1}^{N} g_{ip}^{(2)} W_{2pj} - 2V_x^2 \frac{\partial I_3}{\partial x} \sum_{p=1}^{N} g_{ip}^{(1)} W_{2pj} - V_x^2 \frac{\partial^2 I_3}{\partial x^2} W_{2ij}$$

,

$$\mathcal{K}_{47} = 3D_{55} \sum_{p=1}^{N} g_{ip}^{(1)} U_{3pj} + 3D_{55}^{(1)} \sum_{p=1}^{N} I_{ip} U_{3pj} - D_{13} \sum_{p=1}^{N} g_{ip}^{(1)} U_{3pj},$$

$$\mathcal{K}_{48} = E_{55} \sum_{p=1}^{N} g_{ip}^{(2)} W_{3pj} + E_{55}^{(1)} \sum_{p=1}^{N} g_{ip}^{(1)} W_{3pj} - 3C_{33} W_{3ij} - V_x^2 v - 2V_x^2 \frac{\partial I_4}{\partial x} \sum_{p=1}^{N} g_{ip}^{(1)} W_{3pj} - V_x^2 \frac{\partial^2 I_4}{\partial x^2} W_{3ij}$$

,

$$\mathcal{K}_{51} = C_{11} \sum_{p=1}^{N} g_{ip}^{(2)} U_{0pj} + C_{11}^{(1)} \sum_{p=1}^{N} g_{ip}^{(1)} U_{0pj} - V_x^2 I_2 \sum_{p=1}^{N} g_{ip}^{(2)} U_{0pj} - 2V_x^2 \frac{\partial I_2}{\partial x} \sum_{p=1}^{N} g_{ip}^{(1)} U_{0pj} - V_x^2 \frac{\partial^2 I_2}{\partial x^2} U_{0ij}$$

,

$$\mathcal{K}_{52} = -2B_{55} \sum_{p=1}^{N} g_{ip}^{(1)} W_{0pj},$$

$$\mathcal{K}_{53} =$$
$$D_{11} \sum_{p=1}^{N} g_{ip}^{(2)} U_{1pj} + D_{11}^{(1)} \sum_{p=1}^{N} g_{ip}^{(1)} U_{1pj} - 2B_{55} U_{1ij} - V_x^2 I_3 \sum_{p=1}^{N} g_{ip}^{(2)} U_{1pj} - 2V_x^2 \frac{\partial I_3}{\partial x} \sum_{p=1}^{N} g_{ip}^{(1)} U_{1pj} - V_x^2 \frac{\partial^2 I_3}{\partial x^2} U_{1ij}$$

,

$$\mathcal{K}_{54} = C_{13} \sum_{p=1}^{N} g_{ip}^{(1)} W_{1pj} + C_{13}^{(1)} \sum_{p=1}^{N} I_{ip} W_{1pj} - 2C_{55} \sum_{p=1}^{N} g_{ip}^{(1)} W_{1pj},$$

$$\mathcal{K}_{55} =$$
$$E_{11} \sum_{p=1}^{N} g_{ip}^{(2)} U_{2pj} + E_{11}^{(1)} \sum_{p=1}^{N} g_{ip}^{(1)} U_{2pj} - 4C_{55} U_{2ij} - V_x^2 I_4 \sum_{p=1}^{N} g_{ip}^{(2)} U_{2pj} -$$
$$2V_x^2 \frac{\partial I_4}{\partial x} \sum_{p=1}^{N} g_{ip}^{(1)} U_{2pj} - V_x^2 \frac{\partial^2 I_4}{\partial x^2} U_{2ij}$$
,

$$\mathcal{K}_{56} = 2D_{13} \sum_{p=1}^{N} g_{ip}^{(1)} W_{2pj} + 2D_{13}^{(1)} \sum_{p=1}^{N} I_{ip} W_{2pj} - 2D_{55} \sum_{p=1}^{N} g_{ip}^{(1)} W_{2pj},$$

$$\mathcal{K}_{57} =$$
$$F_{11} \sum_{p=1}^{N} g_{ip}^{(2)} U_{3pj} + F_{11}^{(1)} \sum_{p=1}^{N} g_{ip}^{(1)} U_{3pj} - 6D_{55} U_{3ij} - V_x^2 I_5 \sum_{p=1}^{N} g_{ip}^{(2)} U_{3pj} -$$
$$2V_x^2 \frac{\partial I_5}{\partial x} \sum_{p=1}^{N} g_{ip}^{(1)} U_{3pj} - V_x^2 \frac{\partial^2 I_5}{\partial x^2} U_{3ij}$$
,

$$\mathcal{K}_{58} = 3E_{13} \sum_{p=1}^{N} g_{ip}^{(1)} W_{3pj} + 3E_{13}^{(1)} \sum_{p=1}^{N} I_{ip} W_{3pj} - 2E_{55} \sum_{p=1}^{N} g_{ip}^{(1)} W_{3pj},$$

$$\mathcal{K}_{61} = -2B_{13} \sum_{p=1}^{N} g_{ip}^{(1)} U_{0pj},$$

$$\mathcal{K}_{62} = C_{55} \sum_{p=1}^{N} g_{ip}^{(2)} W_{0pj} + C_{55}^{(1)} \sum_{p=1}^{N} g_{ip}^{(1)} W_{0pj} - V_x^2 I_2 \sum_{p=1}^{N} g_{ip}^{(2)} W_{0pj} - 2V_x^2 \frac{\partial I_2}{\partial x} \sum_{p=1}^{N} g_{ip}^{(1)} W_{0pj} -$$
$$V_x^2 \frac{\partial^2 I_2}{\partial x^2} W_{0ij}$$
,

$$\mathcal{K}_{63} = C_{55} \sum_{p=1}^{N} g_{ip}^{(1)} U_{1pj} + C_{55}^{(1)} \sum_{p=1}^{N} I_{ip} U_{1pj} - 2C_{13} \sum_{p=1}^{N} g_{ip}^{(1)} U_{1pj},$$

$$\mathcal{K}_{64} =$$
$$D_{55} \sum_{p=1}^{N} g_{ip}^{(2)} W_{1pj} + D_{55}^{(1)} \sum_{p=1}^{N} g_{ip}^{(1)} W_{1pj} - 2B_{33} W_{1ij} - V_x^2 I_3 \sum_{p=1}^{N} g_{ip}^{(2)} W_{1pj} -$$
$$2V_x^2 \frac{\partial I_3}{\partial x} \sum_{p=1}^{N} g_{ip}^{(1)} W_{1pj} - V_x^2 \frac{\partial^2 I_3}{\partial x^2} W_{1ij}$$
,

$$\mathcal{K}_{65} = 2D_{55} \sum_{p=1}^{N} g_{ip}^{(1)} U_{2pj} + 2D_{55}^{(1)} \sum_{p=1}^{N} I_{ip} U_{2pj} - 2D_{13} \sum_{p=1}^{N} g_{ip}^{(1)} U_{2pj},$$

$$\mathcal{K}_{66} =$$
$$E_{55} \sum_{p=1}^{N} g_{ip}^{(2)} W_{2pj} + E_{55}^{(1)} \sum_{p=1}^{N} g_{ip}^{(1)} W_{2pj} - 4C_{33} W_{2ij} - V_x^2 I_4 \sum_{p=1}^{N} g_{ip}^{(2)} W_{2pj} -$$
$$2V_x^2 \frac{\partial I_4}{\partial x} \sum_{p=1}^{N} g_{ip}^{(1)} W_{2pj} - V_x^2 \frac{\partial^2 I_4}{\partial x^2} W_{2ij}$$
,

$$\mathcal{K}_{67} = 3E_{55} \sum_{p=1}^{N} g_{ip}^{(1)} U_{3pj} + 3E_{55}^{(1)} \sum_{p=1}^{N} I_{ip} U_{3pj} - 2E_{13} \sum_{p=1}^{N} g_{ip}^{(1)} U_{3pj},$$

$$\mathcal{K}_{68} =$$
$$F_{55} \sum_{p=1}^{N} g_{ip}^{(2)} W_{3pj} + F_{55}^{(1)} \sum_{p=1}^{N} g_{ip}^{(1)} W_{3pj} - 6D_{33} W_{3ij} - V_x^2 I_5 \sum_{p=1}^{N} g_{ip}^{(2)} W_{3pj} -$$
$$2V_x^2 \frac{\partial I_5}{\partial x} \sum_{p=1}^{N} g_{ip}^{(1)} W_{3pj} - V_x^2 \frac{\partial^2 I_5}{\partial x^2} W_{3ij}$$

,

$$\mathcal{K}_{71} = D_{11} \sum_{p=1}^{N} g_{ip}^{(2)} U_{0pj} + D_{11}^{(1)} \sum_{p=1}^{N} g_{ip}^{(1)} U_{0pj} - V_x^2 I_3 \sum_{p=1}^{N} g_{ip}^{(2)} U_{0pj} - 2V_x^2 \frac{\partial I_3}{\partial x} \sum_{p=1}^{N} g_{ip}^{(1)} U_{0pj} - V_x^2 \frac{\partial^2 I_3}{\partial x^2} U_{0ij}$$

,

$$\mathcal{K}_{72} = D_{13}^{(1)} \sum_{p=1}^{N} I_{ip} W_{0pj} - 3C_{55} \sum_{p=1}^{N} g_{ip}^{(1)} W_{0pj},$$

$$\mathcal{K}_{73} = E_{11} \sum_{p=1}^{N} g_{ip}^{(2)} U_{1pj} + E_{11}^{(1)} \sum_{p=1}^{N} g_{ip}^{(1)} U_{1pj} - 3C_{55} U_{1ij} - V_x^2 I_4 \sum_{p=1}^{N} g_{ip}^{(2)} U_{1pj} - 2V_x^2 \frac{\partial I_4}{\partial x} \sum_{p=1}^{N} g_{ip}^{(1)} U_{1pj} - V_x^2 \frac{\partial^2 I_4}{\partial x^2} U_{1ij}$$

,

$$\mathcal{K}_{74} = D_{13} \sum_{p=1}^{N} g_{ip}^{(1)} W_{1pj} + D_{13} \sum_{p=1}^{N} g_{ip}^{(1)} W_{1pj} - 3D_{55} \sum_{p=1}^{N} g_{ip}^{(1)} W_{1pj},$$

$$\mathcal{K}_{75} = F_{11} \sum_{p=1}^{N} g_{ip}^{(2)} U_{2pj} + F_{11}^{(1)} \sum_{p=1}^{N} g_{ip}^{(1)} U_{2pj} - 6D_{55} U_{2ij} - V_x^2 I_5 \sum_{p=1}^{N} g_{ip}^{(2)} U_{2pj} - 2V_x^2 \frac{\partial I_5}{\partial x} \sum_{p=1}^{N} g_{ip}^{(1)} U_{2pj} - V_x^2 \frac{\partial^2 I_5}{\partial x^2} U_{2ij}$$

,

$$\mathcal{K}_{76} = 2E_{13} \sum_{p=1}^{N} g_{ip}^{(1)} W_{2pj} + 2E_{13}^{(1)} \sum_{p=1}^{N} I_{ip} W_{2pj} - 3E_{55} \sum_{p=1}^{N} g_{ip}^{(1)} W_{2pj},$$

$$\mathcal{K}_{77} = G_{11} \sum_{p=1}^{N} g_{ip}^{(2)} U_{3pj} + G_{11}^{(1)} \sum_{p=1}^{N} g_{ip}^{(1)} U_{3pj} - 9E_{55} U_{3ij} - V_x^2 I_6 \sum_{p=1}^{N} g_{ip}^{(2)} U_{3pj} - 2V_x^2 \frac{\partial I_6}{\partial x} \sum_{p=1}^{N} g_{ip}^{(1)} U_{3pj} - V_x^2 \frac{\partial^2 I_6}{\partial x^2} U_{3ij}$$

,

$$\mathcal{K}_{78} = 3F_{13} \sum_{p=1}^{N} g_{ip}^{(1)} W_{3pj} + 3F_{13}^{(1)} \sum_{p=1}^{N} I_{ip} W_{3pj} - 3F_{55} \sum_{p=1}^{N} g_{ip}^{(1)} W_{3pj},$$

$$\mathcal{K}_{81} = -3C_{13} \sum_{p=1}^{N} g_{ip}^{(1)} U_{0pj},$$

$$\mathcal{K}_{82} = D_{55} \sum_{p=1}^{N} g_{ip}^{(1)} W_{0pj} + D_{55}^{(1)} \sum_{p=1}^{N} g_{ip}^{(1)} W_{0pj} - V_x^2 I_3 \sum_{p=1}^{N} g_{ip}^{(2)} W_{0pj} - 2V_x^2 \frac{\partial I_3}{\partial x} \sum_{p=1}^{N} g_{ip}^{(1)} W_{0pj} - V_x^2 \frac{\partial^2 I_3}{\partial x^2} W_{0ij}$$

,

$$\mathcal{K}_{83} = 2E_{55} \sum_{p=1}^{N} g_{ip}^{(1)} U_{2pj} + 2E_{55}^{(1)} \sum_{p=1}^{N} I_{ip} U_{2pj} - 3D_{13} \sum_{p=1}^{N} g_{ip}^{(1)} U_{1pj},$$

$$\mathcal{K}_{84} = E_{55} \sum_{p=1}^{N} g_{ip}^{(1)} W_{1pj} + E_{55}^{(1)} \sum_{p=1}^{N} g_{ip}^{(1)} W_{1pj} - 3C_{33} W_{1ij} - V_x^2 I_4 \sum_{p=1}^{N} g_{ip}^{(2)} W_{1pj} - 2V_x^2 \frac{\partial I_4}{\partial x} \sum_{p=1}^{N} g_{ip}^{(1)} W_{1pj} - V_x^2 \frac{\partial^2 I_4}{\partial x^2} W_{1ij}$$

,

$$\mathcal{K}_{85} = 2E_{55}\sum_{p=1}^{N}g_{ip}^{(1)}U_{2pj} + 2E_{55}^{(1)}\sum_{p=1}^{N}I_{ip}U_{2pj} - 3E_{13}\sum_{p=1}^{N}g_{ip}^{(1)}U_{2pj},$$

$$\mathcal{K}_{86} =$$
$$F_{55}\sum_{p=1}^{N}g_{ip}^{(1)}W_{2pj} + F_{55}^{(1)}\sum_{p=1}^{N}g_{ip}^{(1)}W_{2pj} - 6D_{33}W_{2ij} - V_x^2 I_5\sum_{p=1}^{N}g_{ip}^{(2)}W_{2pj} -$$
$$2V_x^2\frac{\partial I_5}{\partial x}\sum_{p=1}^{N}g_{ip}^{(1)}W_{2pj} - V_x^2\frac{\partial^2 I_5}{\partial x^2}W_{2ij}$$

,

$$\mathcal{K}_{87} = 3F_{55}\sum_{p=1}^{N}g_{ip}^{(1)}U_{3pj} + 3F_{55}^{(1)}\sum_{p=1}^{N}I_{ip}U_{3pj} - 3F_{13}\sum_{p=1}^{N}g_{ip}^{(1)}U_{3pj},$$

$$\mathcal{K}_{88} =$$
$$G_{55}\sum_{p=1}^{N}g_{ip}^{(1)}W_{3pj} + G_{55}^{(1)}\sum_{p=1}^{N}g_{ip}^{(1)}W_{3pj} - 9E_{33}W_{3ij} - V_x^2 I_6\sum_{p=1}^{N}g_{ip}^{(2)}W_{3pj} -$$
$$2V_x^2\frac{\partial I_6}{\partial x}\sum_{p=1}^{N}g_{ip}^{(1)}W_{3pj} - V_x^2\frac{\partial^2 I_6}{\partial x^2}W_{3ij}$$

,

$$\mathcal{M}_{11} = I_0 U_{0ij}, \; \mathcal{M}_{12} = 0, \; \mathcal{M}_{13} = I_1 U_{1ij}, \; \mathcal{M}_{14} = 0,$$
$$\mathcal{M}_{15} = I_2 U_{2ij}, \mathcal{M}_{16} = 0, \mathcal{M}_{17} = I_3 U_{3ij}, \mathcal{M}_{18} = 0,$$
$$\mathcal{M}_{21} = 0, \; \mathcal{M}_{22} = I_0 W_{0ij}, \; \mathcal{M}_{23} = 0, \; \mathcal{M}_{24} = I_1 W_{1ij},$$
$$\mathcal{M}_{25} = 0, \mathcal{M}_{26} = I_2 W_{2ij}, \mathcal{M}_{27} = 0, \mathcal{M}_{28} = I_3 W_{3ij},$$
$$\mathcal{M}_{31} = I_1 U_{0ij}, \; \mathcal{M}_{32} = 0, \; \mathcal{M}_{33} = I_2 U_{1ij}, \; \mathcal{M}_{34} = 0,$$
$$\mathcal{M}_{35} = I_3 U_{2ij}, \mathcal{M}_{36} = 0, \mathcal{M}_{37} = I_4 U_{3ij}, \mathcal{M}_{38} = 0,$$
$$\mathcal{M}_{41} = 0, \; \mathcal{M}_{42} = I_1 W_{0ij}, \; \mathcal{M}_{43} = 0, \; \mathcal{M}_{44} = I_2 W_{1ij},$$
$$\mathcal{M}_{45} = 0, \mathcal{M}_{46} = I_3 W_{2ij}, \mathcal{M}_{47} = 0, \mathcal{M}_{48} = I_4 W_{3ij},$$
$$\mathcal{M}_{51} = I_2 U_{0ij}, \; \mathcal{M}_{52} = 0, \; \mathcal{M}_{53} = I_3 U_{1ij}, \; \mathcal{M}_{54} = 0,$$
$$\mathcal{M}_{55} = I_4 U_{2ij}, \mathcal{M}_{56} = 0, \mathcal{M}_{57} = I_5 U_{3ij}, \mathcal{M}_{58} = 0,$$
$$\mathcal{M}_{61} = 0, \; \mathcal{M}_{62} = I_2 W_{0ij}, \; \mathcal{M}_{63} = 0, \; \mathcal{M}_{64} = I_3 W_{1ij},$$
$$\mathcal{M}_{65} = 0, \mathcal{M}_{66} = I_4 W_{2ij}, \mathcal{M}_{67} = 0, \mathcal{M}_{68} = I_5 W_{3ij},$$
$$\mathcal{M}_{71} = I_3 U_{0ij}, \; \mathcal{M}_{72} = 0, \; \mathcal{M}_{73} = I_4 U_{1ij}, \; \mathcal{M}_{74} = 0,$$
$$\mathcal{M}_{75} = I_5 U_{2ij}, \mathcal{M}_{76} = 0, \mathcal{M}_{77} = I_6 U_{3ij}, \mathcal{M}_{78} = 0,$$
$$\mathcal{M}_{81} = 0, \; \mathcal{M}_{82} = I_3 W_{0ij}, \; \mathcal{M}_{83} = 0, \; \mathcal{M}_{84} = I_4 W_{1ij},$$
$$\mathcal{M}_{85} = 0, \mathcal{M}_{86} = I_5 W_{2ij}, \mathcal{M}_{87} = 0, \mathcal{M}_{88} = I_6 W_{3ij},$$
$$\mathcal{C}_{11} = 2V_x i\omega I_0\sum_{p=1}^{N}g_{ip}^{(1)}U_{0pj} + 2V_x i\omega\frac{\partial I_0}{\partial x}U_{0ij}, \; \mathcal{C}_{12} = 0,$$
$$\mathcal{C}_{13} = 2V_x i\omega I_1\sum_{p=1}^{N}g_{ip}^{(1)}U_{1pj} + 2V_x i\omega\frac{\partial I_1}{\partial x}U_{1ij}, \; \mathcal{C}_{14} = 0,$$
$$\mathcal{C}_{15} = 2V_x i\omega I_2\sum_{p=1}^{N}g_{ip}^{(1)}U_{2pj} + 2V_x i\omega\frac{\partial I_2}{\partial x}U_{2ij}, \mathcal{C}_{16} = 0,$$
$$\mathcal{C}_{17} = 2V_x i\omega I_3\sum_{p=1}^{N}g_{ip}^{(1)}U_{3pj} + 2V_x i\omega\frac{\partial I_3}{\partial x}U_{3ij}, \mathcal{C}_{18} = 0,$$
$$\mathcal{C}_{21} = 0, \; \mathcal{C}_{22} = 2V_x i\omega I_0\sum_{p=1}^{N}g_{ip}^{(1)}W_{0pj} + 2V_x i\omega\frac{\partial I_0}{\partial x}W_{0ij},$$

$$C_{23} = 0, C_{24} = 2V_x i\omega I_1 \sum_{p=1}^{N} g_{ip}^{(1)} W_{1pj} + 2V_x i\omega \frac{\partial I_1}{\partial x} W_{1ij},$$

$$C_{25} = 0, C_{26} = 2V_x i\omega I_2 \sum_{p=1}^{N} g_{ip}^{(1)} W_{2pj} + 2V_x i\omega \frac{\partial I_2}{\partial x} W_{2ij},$$

$$C_{27} = 0, C_{28} = 2V_x i\omega I_3 \sum_{p=1}^{N} g_{ip}^{(1)} W_{3pj} + 2V_x i\omega \frac{\partial I_3}{\partial x} W_{3ij},$$

$$C_{31} = 2V_x i\omega I_1 \sum_{p=1}^{N} g_{ip}^{(1)} U_{0pj} + 2V_x i\omega \frac{\partial I_1}{\partial x} U_{0ij}, C_{32} = 0,$$

$$C_{33} = 2V_x i\omega I_2 \sum_{p=1}^{N} g_{ip}^{(1)} U_{1pj} + 2V_x i\omega \frac{\partial I_2}{\partial x} U_{1ij}, C_{34} = 0,$$

$$C_{35} = 2V_x i\omega I_3 \sum_{p=1}^{N} g_{ip}^{(1)} U_{2pj} + 2V_x i\omega \frac{\partial I_3}{\partial x} U_{2ij}, C_{36} = 0,$$

$$C_{37} = 2V_x i\omega I_4 \sum_{p=1}^{N} g_{ip}^{(1)} U_{3pj} + 2V_x i\omega \frac{\partial I_4}{\partial x} U_{3ij}, C_{38} = 0,$$

$$C_{41} = 0, C_{42} = 2V_x i\omega I_1 \sum_{p=1}^{N} g_{ip}^{(1)} W_{0pj} + 2V_x i\omega \frac{\partial I_1}{\partial x} W_{0ij},$$

$$C_{43} = 0, C_{44} = 2V_x i\omega I_2 \sum_{p=1}^{N} g_{ip}^{(1)} W_{1pj} + 2V_x i\omega \frac{\partial I_2}{\partial x} W_{1ij},$$

$$C_{45} = 0, C_{46} = 2V_x i\omega I_3 \sum_{p=1}^{N} g_{ip}^{(1)} W_{2pj} + 2V_x i\omega \frac{\partial I_3}{\partial x} W_{2ij},$$

$$C_{47} = 0, C_{48} = 2V_x i\omega I_4 \sum_{p=1}^{N} g_{ip}^{(1)} W_{3pj} + 2V_x i\omega \frac{\partial I_4}{\partial x} W_{3ij},$$

$$C_{51} = 2V_x i\omega I_2 \sum_{p=1}^{N} g_{ip}^{(1)} U_{0pj} + 2V_x i\omega \frac{\partial I_2}{\partial x} U_{0ij}, C_{52} = 0,$$

$$C_{53} = 2V_x i\omega I_3 \sum_{p=1}^{N} g_{ip}^{(1)} U_{1pj} + 2V_x i\omega \frac{\partial I_3}{\partial x} U_{1ij}, C_{54} = 0,$$

$$C_{55} = 2V_x i\omega I_4 \sum_{p=1}^{N} g_{ip}^{(1)} U_{2pj} + 2V_x i\omega \frac{\partial I_4}{\partial x} U_{2ij}, C_{56} = 0,$$

$$C_{57} = 2V_x i\omega I_5 \sum_{p=1}^{N} g_{ip}^{(1)} U_{3pj} + 2V_x i\omega \frac{\partial I_5}{\partial x} U_{3ij}, C_{58} = 0,$$

$$C_{61} = 0, C_{62} = 2V_x i\omega I_2 \sum_{p=1}^{N} g_{ip}^{(1)} W_{0pj} + 2V_x i\omega \frac{\partial I_2}{\partial x} W_{0ij},$$

$$C_{63} = 0, C_{64} = 2V_x i\omega I_3 \sum_{p=1}^{N} g_{ip}^{(1)} W_{1pj} + 2V_x i\omega \frac{\partial I_3}{\partial x} W_{1ij},$$

$$C_{65} = 0, C_{66} = 2V_x i\omega I_4 \sum_{p=1}^{N} g_{ip}^{(1)} W_{2pj} + 2V_x i\omega \frac{\partial I_4}{\partial x} W_{2ij},$$

$$C_{67} = 0, C_{68} = 2V_x i\omega I_5 \sum_{p=1}^{N} g_{ip}^{(1)} W_{3pj} + 2V_x i\omega \frac{\partial I_5}{\partial x} W_{3ij},$$

$$C_{71} = 2V_x i\omega I_3 \sum_{p=1}^{N} g_{ip}^{(1)} U_{0pj} + 2V_x i\omega \frac{\partial I_3}{\partial x} U_{0ij}, C_{72} = 0,$$

$$C_{73} = 2V_x i\omega I_4 \sum_{p=1}^{N} g_{ip}^{(1)} U_{1pj} + 2V_x i\omega \frac{\partial I_4}{\partial x} U_{1ij}, C_{74} = 0,$$

$$C_{75} = 2V_x i\omega I_5 \sum_{p=1}^{N} g_{ip}^{(1)} U_{2pj} + 2V_x i\omega \frac{\partial I_5}{\partial x} U_{2ij}, C_{76} = 0,$$

$$C_{57} = 2V_x i\omega I_6 \sum_{p=1}^{N} g_{ip}^{(1)} U_{3pj} + 2V_x i\omega \frac{\partial I_6}{\partial x} U_{3ij}, C_{58} = 0,$$

$$C_{61} = 0, C_{62} = 2V_x i\omega I_3 \sum_{p=1}^{N} g_{ip}^{(1)} W_{0pj} + 2V_x i\omega \frac{\partial I_3}{\partial x} W_{0ij},$$

$$C_{83} = 0, C_{84} = 2V_x i\omega I_4 \sum_{p=1}^{N} g_{ip}^{(1)} W_{1pj} + 2V_x i\omega \frac{\partial I_4}{\partial x} W_{1ij},$$

$$C_{85} = 0, C_{86} = 2V_x i\omega I_5 \sum_{p=1}^{N} g_{ip}^{(1)} W_{2pj} + 2V_x i\omega \frac{\partial I_5}{\partial x} W_{2ij},$$

$$C_{87} = 0, C_{88} = 2V_x i\omega I_6 \sum_{p=1}^{N} g_{ip}^{(1)} W_{3pj} + 2V_x i\omega \frac{\partial I_6}{\partial x} W_{3ij}.$$

REFERENCES

[1]   Sekkal M, Bouiadjra RB, Benyoucef S, Tounsi A, Ghazwani MH, Alnujaie A. Effect of material distribution on bending and buckling response of a bidirectional FG beam exposed to a combined transverses and variable axially loads. *Mechanics Based Design of Structures and Machines* 2023;0:1–20. https://doi.org/10.1080/15397734.2023.2172032.

[2]   Chami GMB, Kahil A, Hadji L. Influence of porosity on the fundamental natural frequencies of FG sandwich beams. *Materials Today: Proceedings* 2022;53:107–12.

[3]   Zhao S, Zhang Y, Zhang Y, Yang J, Kitipornchai S. Vibrational characteristics of functionally graded graphene origami-enabled auxetic metamaterial beams based on machine learning assisted models. *Aerospace Science and Technology* 2022;130:107906.

[4]   Liu Z, Yan X, Qi M, Huang D, Zhang X, Lin L. Electrostatic flapping-wing actuator with improved lift force by the pivot-spar bracket design. *Sensors and Actuators A: Physical* 2018;280:295–302.

[5]   Bouzidi I, Hadjoui A, Fellah A. Dynamic analysis of functionally graded rotor-blade system using the classical version of the finite element method. *Mechanics Based Design of Structures and Machines* 2021;49:1080–108.

[6]   Murari B, Zhao S, Zhang Y, Yang J. Static and dynamic instability of functionally graded graphene origami-enabled auxetic metamaterial beams with variable thickness in fluid. *Ocean Engineering* 2023;280:114859.

[7]   Zhou X, Jing L. Large deflection response of sandwich beams with layered-gradient foam cores subjected to low-velocity impact. *International Journal of Impact Engineering* 2023;172:104429.

[8]   Pradhan N, Sarangi S. Analysis of functionally graded beams subjected to Thermo-mechanical loading using finite element method. *Materials Today: Proceedings* 2018;5:19490–6.

[9]   Kar UK, Srinivas J. Vibration analysis of Bi-directional FG-GNPs reinforced rotating micro-beam under Thermo-mechanical loading. *Materials Today: Proceedings* 2023;78:752–9.

[10]   Meksi A, Sekkal M, Bouiadjra RB, Benyoucef S, Tounsi A. Assessing the effect of temperature-dependent properties on the dynamic behavior of FG porous beams rested on variable elastic foundation. *Structural Engineering and Mechanics* 2023;85:717.

[11]   Jiang F, Ding Y, Song Y, Geng F, Wang Z. CFRP strengthening of fatigue cracks at U-rib to diaphragm welds in orthotropic steel bridge decks: *Experimental study, optimization, and decision-makin*g. vol. 43, Elsevier; 2022, p. 1216–29.

[12]   Pang F, Gao C, Li H, Jia D, Wang X, Miao X. Vibration analysis of FG beams under arbitrary load with general boundary conditions: *Theoretical and experimental comparative research. Thin-Walled Structures* 2022;179:109605.

[13]   Simonetti SK, Turkalj G, Lanc D. Thermal buckling analysis of thin-walled closed section FG beam-type structures. *Thin-Walled Structures* 2022;181:110075.

[14]   Genel ÖE, Tüfekci E. Bending-bending coupled static analysis of functionally graded and porous pretwisted cantilever beams using initial values method. *Mechanics Based Design of Structures and Machines* 2023;0:1–24. https://doi.org/10.1080/15397734.2023.2185632.

[15]   Wu K, Liu Z, Ding Q, Gu F, Ball A. Torsional vibration responses of the engine crankshaft-gearbox coupled system with misfire and breathing slant crack based on instantaneous angular speed. *Mechanical Systems and Signal Processing* 2022;173:109052.

[16]   Scheidl J, Vetyukov Y. Review and perspectives in applied mechanics of axially moving flexible structures. *Acta Mechanica* 2023;234:1331–64.

[17]   Phi LT, Nguyen T-T, Kang J, Lee J. Vibration and buckling optimization of thin-walled functionally graded open-section beams. *Thin-Walled Structures* 2022;170:108586.

[18]   Zhang L, Xu Z, Gao M, Xu R, Wang G. Static, dynamic and buckling responses of random functionally graded beams reinforced by graphene platelets. *Engineering Structures* 2023;291:116476.

[19]   Hirannaiah S, Swaminathan K, Rajanna T. Thermo-mechanical vibration and buckling analysis of porous FG sandwich plates with geometric discontinuity based on physical neutral surface. *Mechanics of Advanced Materials and Structures* 2023:1–25.

[20]   Alsheyab MA, Khasawneh MA. Evaluating fatigue performance of Bailey asphalt mixtures containing natural river sand at varied strain and air void levels. *Mechanics of Advanced Materials and Structures* 2023:1–12.

[21]   Abo-Bakr H, Abo-Bakr R, Mohamed S, Eltaher M. Weight optimization of axially functionally graded microbeams under buckling and vibration behaviors. *Mechanics Based Design of Structures and Machines* 2023;51:213–34.

[22]   Li C, Shen H-S, Yang J. Design and nonlinear dynamics of FG curved sandwich beams with self-adapted auxetic 3D double-V meta-lattice core. *Engineering Structures* 2022;272:115023.

[23]   Momeni S, Zabihollah A, Behzad M. Effects of size and location of magnetorheological segments on random vibration response of laminated composite beams using an N-layer of layerwise theory. *Journal of Thermoplastic Composite Materials* 2023:08927057231154427.

[24]   Murari B, Zhao S, Zhang Y, Yang J. Graphene origami-enabled auxetic metamaterial tapered beams in fluid: Nonlinear vibration and postbuckling analyses via physics-embedded machine learning model. *Applied Mathematical Modelling* 2023.

[25]   Lezgy-Nazargah M, Karamanli A, Vo TP. Bending, buckling and free vibration analyses of shallow-to-deep FG curved sandwich beams using a global–local refined shear deformation theory. vol. 52, Elsevier; 2023, p. 568–81.

[26]   Yapicioglu A, Dincer I. A newly developed renewable energy driven multigeneration system with hot silica sand storage for power, hydrogen, freshwater and cooling production. *Sustainable Energy Technologies and Assessments* 2023;55:102938.

[27]   Palmquist A, Jolic M, Hryha E, Shah FA. Complex geometry and integrated macro-porosity: Clinical applications of electron beam melting to fabricate bespoke bone-anchored implants. *Acta Biomaterialia* 2023;156:125–45.

[28]   Rouf S, Malik A, Raina A, Haq MIU, Naveed N, Zolfagharian A, et al. Functionally graded additive manufacturing for orthopedic applications. *Journal of Orthopaedics* 2022;33:70–80.

[29]   Lee J-H, Lee H-L, Park I-Y, On S-W, Byun S-H, Yang B-E. Effectiveness of creating digital twins with different digital dentition models and cone-beam computed tomography. *Scientific Reports* 2023;13:10603.

[30]   Bazmara M, Silani M, Mianroodi M. Physics-informed neural networks for nonlinear bending of 3D functionally graded beam. vol. 49, *Elsevier*; 2023, p. 152–62.

[31]   Nguyen-Xuan H, Tran KQ, Thai CH, Lee J. Modelling of functionally graded triply periodic minimal surface (FG-TPMS) plates. *Composite Structures* 2023;315:116981.

[32]   Goker F, Russillo A, Baj A, Giannì A, Beltramini G, Rossi D, et al. Custom made/patient specific alloplastic total temporomandibular joint replacement in immature patient: a case report and short review of literature. *European Review for Medical and Pharmacological Sciences* 2022;26:26–34.

[33]   Tabarrok B, Leech C, Kim Y. On the dynamics of an axially moving beam. *Journal of the Franklin Institute* 1974;297:201–20.

[34]   Kong L, Parker R. Approximate eigensolutions of axially moving beams with small flexural stiffness. *Journal of Sound and Vibration* 2004;276:459–69.

[35]   Öz H, Pakdemirli M, Boyacı H. Non-linear vibrations and stability of an axially moving beam with time-dependent velocity. *International Journal of Non-Linear Mechanics* 2001;36:107–15.

[36]   Beni YT. Size dependent coupled electromechanical torsional analysis of porous FG flexoelectric micro/nanotubes. *Mechanical Systems and Signal Processing* 2022;178:109281.

[37]   Beni ZT, Beni YT. Dynamic stability analysis of size-dependent viscoelastic/piezoelectric nano-beam. *International Journal of Structural Stability and Dynamics* 2022;22:2250050.

[38]   Sze K, Chen S and, Huang J. The incremental harmonic balance method for nonlinear vibration of axially moving beams. *Journal of Sound and Vibration* 2005;281:611–26.

[39]   Chen S, Huang J, Sze K. Multidimensional Lindstedt–Poincaré method for nonlinear vibration of axially moving beams. *Journal of Sound and Vibration* 2007;306:1–11.

[40]   Ding H, Chen L-Q. Natural frequencies of nonlinear vibration of axially moving beams. *Nonlinear Dynamics* 2011;63:125–34.

[41]   Karimipour I, Beni YT. Nonlinear dynamic analysis of nonlocal composite laminated toroidal shell segments subjected to mechanical shock. *Communications in Nonlinear Science and Numerical Simulation* 2022;106:106105.

[42]   Larbi LO, Kaci A, Houari MSA, Tounsi A. An efficient shear deformation beam theory based on neutral surface position for bending and free vibration of functionally graded beams#. *Mechanics Based Design of Structures and Machines* 2013;41:421–33.

[43]   Şimşek M. Buckling of Timoshenko beams composed of two-dimensional functionally graded material (2D-FGM) having different boundary conditions. Composite Structures 2016;149:304–14. https://doi.org/10.1016/j.compstruct.2016.04.034.

[44]   Reddy J, Chin C. Thermomechanical analysis of functionally graded cylinders and plates. *Journal of Thermal Stresses* 1998;21:593–626.

[45]   Sadd MH. Elasticity: theory, applications, and numerics. *Academic Press*; 2009.

[46]   Miraliyari O, Jafari Mehrabadi S, Najafizadeh M. Nonlinear Free Vibration Analysis of Functionally Graded Sandwich Beam with Magnetorheological Fluid Core Using Timoshenko Beam Theory. *Journal of Solid Mechanics* 2023;15:120–43.

[47]   Ghorbanpour Arani A, Pakize M, Irani Rahaghi M, Khoddami Maraghi Z, Niknejad S. Vibrational Study on Multilayer Sandwich Plates: Porous FGM Core, Nanocomposite and Piezoelectric Face Sheets. *Journal of Solid Mechanics* 2022.

[48]   Karbasizadeh A, Ghorbanpour Arani A, Niknejad S, Khoddami Maraghi Z. Free Damped Vibration Analysis of Sandwich Plates with CNT-Reinforced MRE Core and Laminated Three-Phase Polymer/GPL/Fiber Face Sheets. *Journal of Solid Mechanics* 2023.

[49]   Mihankhah A, Khoddami Maraghi Z, Ghorbanpour Arani A, Niknejad S. Vibrations of Multi-layer Beam with Nanocomposite face sheets Reinforced with Graphene Platelets and Porous Core. *Journal of Solid Mechanics* 2023.

[50]   Khosravi M, Jafari Mehrabadi S, Malekzadeh Fard K. Vibration Behavior of Thick Sandwich Composite Beam with Flexible Core Resting on Incompressible Fluid Foundation. *Journal of Solid Mechanics* 2023;15:50–65.

[51]   Tornabene F, Fantuzzi N, Ubertini F, Viola E. Strong formulation finite element method based on differential quadrature: a survey. *Applied Mechanics Reviews* 2015;67.

[52]   Şimşek M. Bi-directional functionally graded materials (BDFGMs) for free and forced vibration of Timoshenko beams with various boundary conditions. *Composite Structures* 2015;133:968–78. https://doi.org/10.1016/j.compstruct.2015.08.021.